Flame propagation in a transparent pipe with a single obstruction

André Vagner Gaathaug

4. June 2008

Abstract

This report treats the problem of hydrogen explosions. The background for this thesis was based upon earlier work done by Bjerketvedt D., Vægsæther K. and Knudsen V. They investigated hydrogen explosions in a steel pipe with a single obstacle.

Literature research of flame acceleration and detonation has been done, and later related to the experiments and simulations. The literature study investigates laminar flames and instability mechanisms. Turbulent flames are studied and described with the Borghi diagram. The literature study ends with detonation deflagration transition (DDT).

Experiments with hydrogen explosions in a 1 m. long and 97 mm. inner diameter transparent pipe with one open end and ignition at the closed end where conducted at Telemark University College. The pipe had one obstacle. The transparent pipe allowed high speed filming of the experiments and revealed inversion of the flame before it hit the obstacle, which confirmed earlier work. There was also a clear linkage between pressure waves reflecting of the obstacle and a halted propagation and inversion of the flame.

An initiation mechanism of flame inversion caused by pressure waves propagating at different velocity in products and reactants is proposed. It is also proposed that pressure waves interacting with inverted flames collapse the inversion.

CFD simulation, using an in house code, of the process of flame inversion was done and they reproduced the proposed mechanism. The simulations revealed that pressure waves propagating from reactants to products both inverted a convex flame and collapsed an inverted flame.

A draft of a scientific paper is written on the topic of flame inversion and included in the appendix. The paper focus on the proposed mechanism and the simulations.

Further work regarding hydrogen explosions in a pipe with a single obstacle is also proposed in the conclusion.

Contents

Chapter 1

Preface

This work has been carried out at Telemark University College. The work is written without any long mathematical derivations and complex models. The work breifly describes the different topics, preferably with descriptive figures. The content of this thesis assumes the reader has a background in basic chemestry and fluid dynamics.

I want to thank my supervisor prof. Dag Bjerketvedt for excellent guidance as well as motivation and humor. The work with this thesis has been a joy, though sometimes a bit lonely. I also want to thank Ph. D. students Ole Kristian Sommersel and Kanchan Rai for great support, teaching and help. I want to thank divisional engineer Talleiv Skredtveit for his contribution of making the experimental equipment. Thanks to the girls at the library for great assistance finding papers and books from all over the world.

To my mentor for the last five years I want to thank Knut Vågsæther. He convinced me to become an engineer and has supported me and helped me through every cource and coffee break since the summer of 2003. Without his help I wouldn't have written this thesis at all.

Porsgrunn, 2008
André Vagner Gaathaug

Chapter 2

Introduction

This report treats the issue of premixed flame propagation in a circular pipe. Pipes are essential equipment in many industries and likely sources of fires and explosions. A circular pipe is also well suited for laboratory scale experiments. The gas mixture used in this report is hydrogen and air at various concentrations. Hydrogen is a well suited gas for laboratory experiments since water is almost the only combustion product. Hydrogen is also a popular energy carrier for future transit systems. There are cars running on hydrogen and research of supersonic airplanes using hydrogen combustion as propulsion agent [24]. In the current debate regarding climate gases such as CO_2, hydrogen is considered a possible solution if the production of hydrogen could be free of CO_2. There are certain dangers regarding the use of hydrogen, such as fires and explosions. Hydrogen explosions have the possibility of severe consequences due to high pressure and blast waves with following flying debris.

The tasks given for this report was:

- A study of hydrogen flame propagation in tubes with obstacles shall be performed to achieve knowledge about the phenomena, and experimental data for verification of a CFD code.
- The candidate will make a literature study of flame acceleration and DDT (Detonation Deflagration Transition).
- CFD analysis of selected experiments shall be done to verify the CFD code.
- A draft of a scientific paper shall be written about the topic, covering the experiments and the simulations.

The experimental study shall investigate how a flame propagates in a 1m long tube with an obstacle in the end, see figure 2.1. Special emphasize will be given to the phenomena of flame inversion. Earlier simulations of flame propagation in a similar tube revealed several flame inversions in the first meter of the pipe, [1]. Detailed investigation of the phenomena of inversion should clarify the mechanisms which cause inversion. Referring experiments to simulations and vice versa is the preferred method of detailed investigation. Simulations can be a good method of isolating different effects.

Figure 2.1: Picture of the setup used in the experiments for this report.

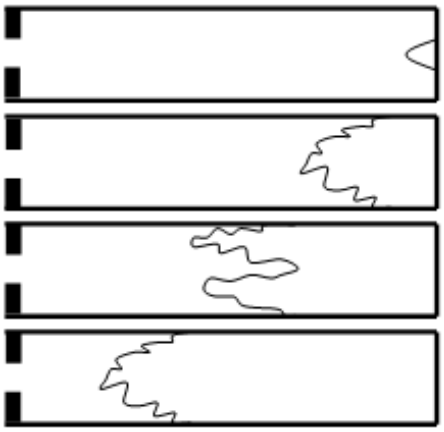

Figure 2.2: The flame propagation is assumed to start off laminar, wrinkle and invert, then it's assumed to collapse and become a turbulent convex flame again. This might happen several times during the propagation through the pipe.

There are many studies of flame propagation in pipes done before, with many different foci. A short and brief description of selected studies will be given in the report without detailed mathematical description of the topics. A lot of background and theory is referred to the doctoral thesis of Vegeir Knudsen (2007) [2], where he investigated hydrogen explosions in pipelines.

A draft paper governing the flame inversion in the pipe shall be written, where simulations and experiments are compared and discussed.

The assumed propagation of the flame in the pipe is given in figure 2.2.

Chapter 3

Flame acceleration - background and theory

Flame propagation in pipes has long been studied and investigated. Many methods of information recording has been used, ranging from pressure records and temperature to high speed filming with and without Schlieren method. Many different gases has been used for study of flame propagation in pipes.

Gas explosions have the potential of devastating consequences, both to people and structures. Keeping this in mind it's important to take measures to prevent loss of life and structural failure due to gas explosions. One way of finding safety measures is to do experiments, but large scale experiments are often very expensive or even impossible. Computer simulated explosions is a cheap and effective way of analyzing safety aspects related to possible gas explosions. The simulation methods are called Computational Fluid Dynamics CFD, and are basically methods of solving discretized partial differential equations. Other sub models are also included in CFD methods, for example models for calculating states or calculating reaction rates. Most sub models are simplifications and, among other factors, sources to errors or inaccuracies. There are always need to verify CFD codes to check their accuracies. Lab scale experiments are cheap and easy ways to verify CFD codes.

This main thesis focuses on flame propagation in a transparent circular plastic pipe. The pressure from the different experiments was recorded. High speed films of the flame propagation was made, but due to circular geometry the schlieren photograph method was not useful. The gas used in the experiments was hydrogen and air at atmospheric pressure. One goal with the experiments was to film the flame propagation in the pipe and compare with CFD simulations. One particular phenomena of interest was the inversion of the flame front. Simulations showed that the center of the flame front moved in opposite direction of the edge of the flame front. This phenomena was believed to be caused by pressure waves interacting with the flame.

Markstein [30] did experiments with shock tube and propagating flames in a 3- by 3-in. square channel. The gas used was butan-air mixture at various concentration. The gas was ignited and after a time delay the membrane in the shock tube was ruptured. The shock propagated towards the flame, and the pressure ratio was 1.3 and 1.6. Schlieren photography of the experiment

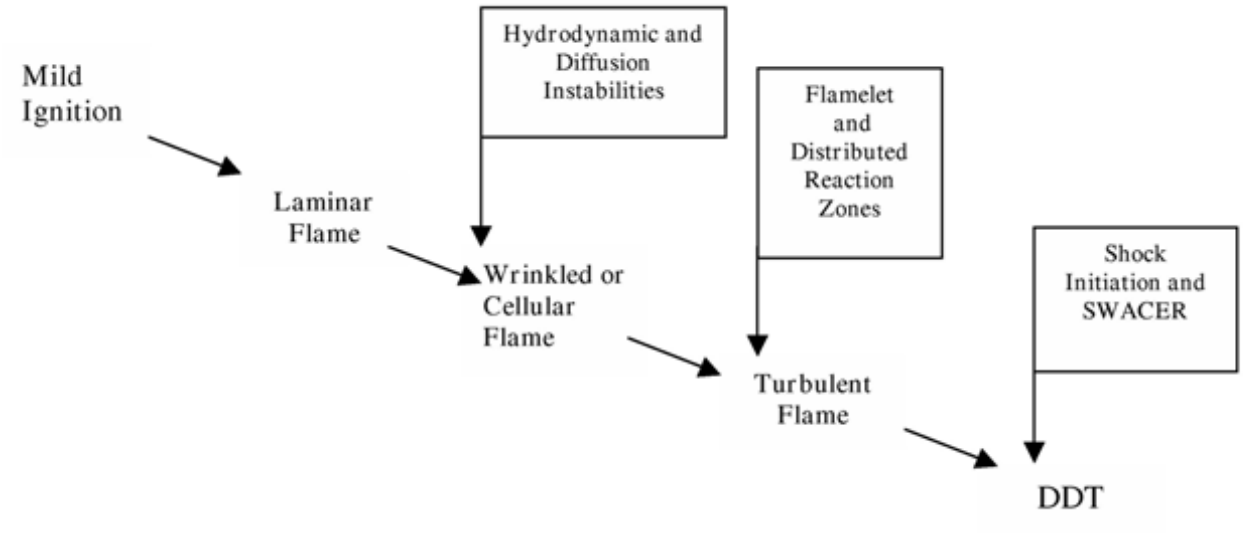

Figure 3.1: The cascade following the flame development from ignition until DDT. [2].

showed that the flame was laminar when the shock passed through the flame, but the flame front inverted and created a funnel of reactants in the middle of the channel.

Teerling et. al. [29] simulated a slightly perturbated flame influenced by oscillatory pressure waves propagating from the products through the flame. They showed that the structure of the flame front oscillated in harmony with the pressure waves. The simulations showed that the flame alternated between creating funnels into the reactants and into the products. A detailed mechanism of the funnel creation was not given.

The development of flame acceleration is sketched in figure 3.1. The flame starts off with an ignition, and propagates as a laminar flame. Different types of instability mechanisms will influence the laminar flame. These are briefly discussed in this chapter. An unstable flame will become turbulent, and turbulent premixed flames are discussed and related to the Borghi diagram. Flames will produce pressure waves which in turn might interacts with the flame. Pressure waves might cause a transition to detonation. Turbulent flames with wrinkled flame front can also be a cause of DDT. A brief discussion of DDT is given in the end of this chapter.

3.1 Flame propagation

Propagation of flames often follow the same pattern, and subsonic combustion waves are often called deflagrations. All flame propagations require flammable gas and oxidizer, usually air or pure oxygen. An ignition is required and can be many different sources. An electric spark or hot surface can be likely ignition sources. After ignition the flame usually propagate laminar as a sphere until

it reaches a solid wall. The flame quenches when it reaches a solid wall, but the flame continues to propagate through unburned reactants. At this point the flame is laminar and propagates with the laminar flame speed. The burning rate is the rate at which heat is released or reactants is burned. It can be defined as following for a stationary flame.

$$\dot{m} = S_L \ A_f \ \rho_u = v_u \ A_f \ \rho_u = v_b \ A_f \ \rho_b$$

Where $\dot{m}$ is the mass rate of either reactants or products. S_L is the laminar flame speed, A_f is the flame area and ρ is density. Since the density of products are lower than the density of reactants the velocity in the products v_b must be higher than the velocity of the reactants. The case where $v_u = S_L$ is where the reactants are stationary. The burning rate is dependent on the flame area. After ignition the flame propagates as a sphere with large surface area relative to the volume of the burned products, when the flame quenches at solid wall the surface area is decreased and the burning rate is lower. This initial unsteady burning rate might cause instabilities later. The laminar flame propagates, and under the influence of instabilities, boundary conditions and boundary layers the flame area varies and burning rate changes leading to instabilities and wrinkling of the flame front. Turbulent flame have wrinkled flame fronts and increased flame area causing high burning rates. Increased burning rates will in turn enhance the turbulence which further increases the burning rate. This positive feedback loop might cause detonation deflagration transition (DDT). See figure 3.1.

3.2 Flame instability - brief description

Following the pathway of figure 3.1, the next step after ignition and laminar flame is influence of instabilities and wrinkling of the flame front. There are several different types of instability mechanisms proposed in the literature. The following instabilities presented are what was believed to be of importance in experiments and simulations.

Many factors will influence propagation of premixed flames, it could be pressure waves, heat loss, obstacles, boundary conditions and many more. Several types of flame instabilities are discussed in the literature, and extensive research is done on that field of science. Instabilities could be seen as pertubations which lead to change in flame property, contradicting stable flames which return to original properties after small perturbations. The following instabilities are referred to in [2]. Detailed description of the different instabilities and their physical description and derivations is considered beyond the scope of this report.

3.2.1 Thermal-diffusive

This type of instability is best described using the dimensionless Lewis number. The Lewis number is the ratio of thermal and molecular diffusivity.

$$Le = \frac{\lambda}{D \ \rho \ c_p}$$

Where λ is the heat conductivity, D is the molecular diffusivity, ρ is the density and c_p is the constant pressure heat capacity. If $Le = 1$ then the heat loss due

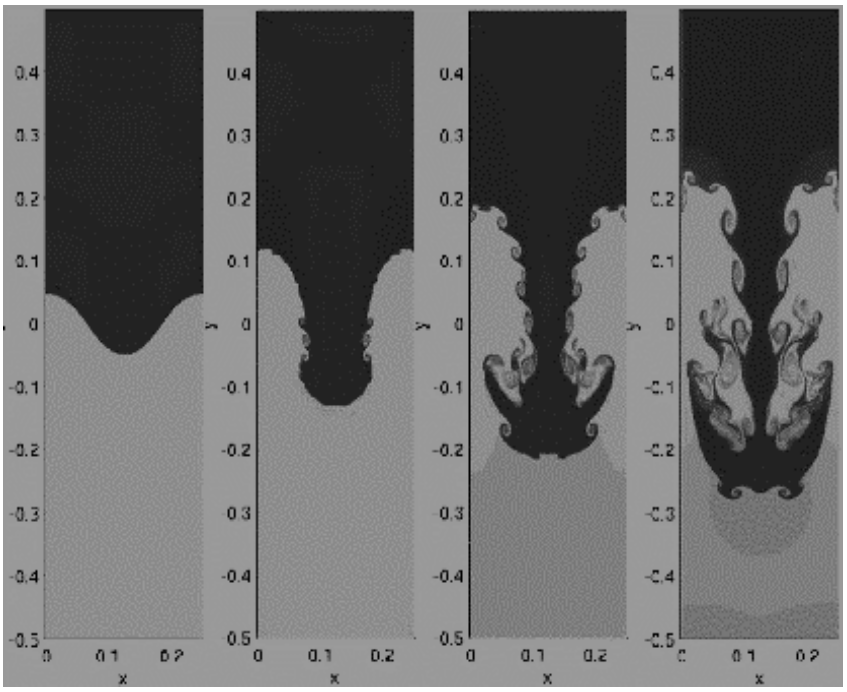

Figure 3.2: Illustration of Rayleigh Taylor instabilities. [25]

to conductivity from the flame and molecular transport into the flame from the reactants is equal. $Le = 1$ is a stable situation. $Le > 1$ implies that the heat conduction is greater than the molecular transport. Then the flame has a deficit feed of reactants and a higher rate of heat loss due to conduction. This situation will cool the flame. It will likely reduce the flame speed and burning rate slowing the whole process down. $Le > 1$ is not considered as a unstable situation due to the reduction of burning rates and flame speed. $Le < 1$ will lead to increased flame temperature due to higher rate of reactant transport into the flame than heat loss from the flame. This situation is considered unstable [2].

3.2.2 Rayleigh-Taylor instabilities

These instabilities are related to acceleration of light fluid into denser fluid. When a light fluid is forced to push a heavy fluid, the interface between the two fluids will be unstable. The light fluid could form fingers into the dense fluid and eventually form mushroom cap at the end. Figure 3.2 shows how a light fluid on top is accelerated into the dense fluid on bottom. In combustion relation Rayleigh-Taylor instabilities can be expected when the light products are accelerated into the denser reactants. The opposite case where dense fluid is accelerated into the lighter fluid is considered stable. [2].

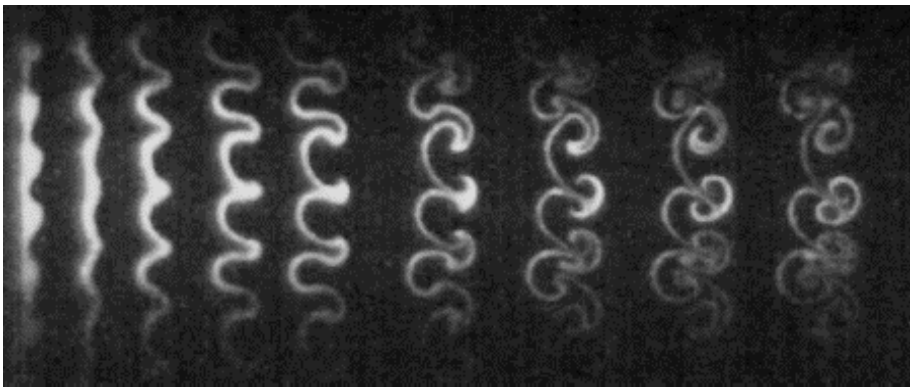

Figure 3.3: Picture showing the Richtmyer-Meshkov instabilities. The light colors are a gas curtain of SF6 with small fog droplets. Picture taken from [3].

3.2.3 Richtmyer-Meshkov instabilities

This instability is closely related to the Rayleigh-Taylor instability. Richtmyer-Meshkov instabilities occur when the interphase between two different density fluids has an impulsive acceleration. This type of acceleration is typical for shock waves. Contradicting the Rayleigh-Taylor instability the instability generated by impulsive accelerations generates unstable interphases both when light is accelerated into dense and opposite. Figure 3.3 is taken from the web site "Mushrooms+Snakes a visualization of Richtmyer-Meshkov instabilities" [3]. The impulsive acceleration is generated from Mach 1.2 shocks.

3.2.4 Kelvin-Helmholtz instability

Kelvin-Helmholtz instability can occur in the shear between to fluids in parallel motion. The difference in velocity of the fluids must be sufficiently large enough and in the presence of a perturbation. The shear between the fluids will make the interphase between them unstable in most cases. The generation of waves on water due to wind is a classic example of Kelvin-Helmholtz instabilities. Figure 3.4 shows how shear layers of clouds generate Kelvin-Helmholtz instabilities. [4].

Kelvin-Helmholtz instabilities can occur in the experiments when the reactants creates a funnel into the flame.

3.2.5 Landau-Darrieus instability

Landau-Darrieus instability govern the instability of curved flames. It's is believed to be of great importance to the experiments and simulations in this report. In basic a curved flame will be stable as long it's convex towards the reactants. If the curvature is changed the flame area will increase. Let's consider a curved flame with a uniform flow field in front. The analysis is semi incompressible stating that the only change of density is across the flame. There is also assumed constant pressure across the flame. Figure 3.5 shows how flowlines converge and diverge in front of a non planar flame.As long as the flow

Figure 3.4: Kelvin-Helmholtz instabilities in the natures own shear layers. Picture taken from [4].

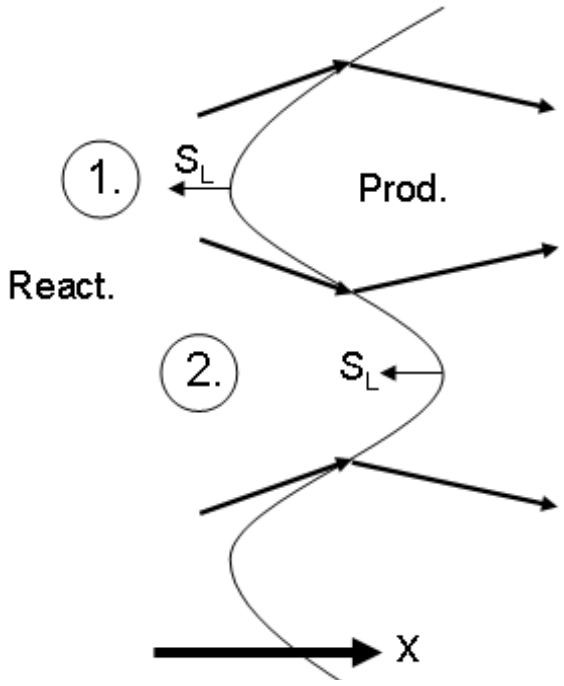

Figure 3.5: The flow field in front of a flame with concave and convex parts.

is considered semi incompressible, the flow velocity at 1. is lower than at 2., given that the flowline diverge at 1. and converge at 2.. If the center line of the wavy perturbation is considered stationary, and the flame burns with the laminar burning velocity relative to the flame, the burning speed at 1. will be:

$$S_{1B} = u_1 - S_L$$

and at 2. it will be:

$$S_{2B} = u_2 - S_L$$

If $u_2 > u_1$ then $S_{2B} > S_{1B}$ hence the flame will move right at 2. and left at 1.. This will increase the curvature and might lead to creation of an inverted flame front.

3.3 Turbulent flames - The Borghi diagram

A wrinkled and unstable flame front could cause variations on flow and flame area, and there is a vague difference between a laminar though unstable flame and a turbulent flame. Figure 3.1, shows that the next step of the flame cascade is flamlet and distributed reaction zones. It is turbulent flames, and one tool for understanding different regimes of turbulent flames is the Borghi diagram.

Turbulence will influence flames in many different ways, but it's highly a matter of length scales of both the flame and the turbulence. Figure 3.6 shows how different length scales of the turbulence influence an ink spot in water. Series a) has large scale eddies and the result is that the ink spot is stretched, since the ink spot is much smaller than the length of the eddies. Series b) has an ink spot much bigger than the turbulent eddies which result in a wrinkling of the ink spot. Similarities to flames will show that if the turbulent eddies are larger than the flame thickness the flame will be stretched, but if the flame thickness is larger than the eddies the flame will be wrinkled and thicker. For more detailed information of turbulent combustion see Peters N. (2000) [7].

Turbulent length scales vary in length and are distributed from the largest to the smallest in a system. The largest eddies evaluated in the theory of turbulent combustion is the integral length l_0. The integral length is defined as

$$l_0(t) = \int_0^\infty f(t,r)dr$$

Where $f(t,r)$ is the correlation between velocities in a turbulent regime at distance r. The description of $f(t,r)$ is not considered in this report, but the integral length is regarded as the large scale of turbulent eddies. Kolmogorov's eddy cascade hypothesis assumes that energy of the largest turbulent eddies is transferred to smaller eddies down to the smallest eddies which is consumed by viscous dissipation. [7]. The smallest length scale of the turbulent eddies is known as the Kolmogorov length scale η. These two length scales are essential in defining turbulent flow, but also the root mean square velocity fluctuations of the turbulent eddies u' (i.e. turbulent intensity) is considered. Length scales

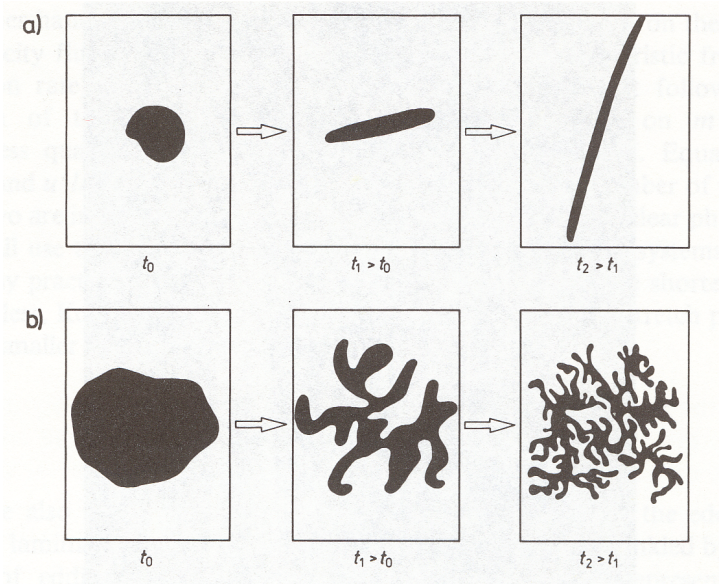

Figure 3.6: How turbulence influence an ink spot in water. Series a) shows large turbulent eddies stretch the ink spot, while b) shows how small eddies wrinkle the ink spot. [6]

and velocities also defines characteristic times of the turbulent flow, as integral time:

$$\tau_{l_0} = \frac{l_0}{u'(l_0)}$$

and the Kolmogorov time as

$$\tau_\eta = \frac{\eta}{u'(\eta)}$$

So far the presented length scales, velocities and time scales are properties of the turbulence. There are also properties describing the flame. The laminar flame speed S_L and the laminar flame thickness δ_L are used to define the chemical time as:

$$\tau_c = \frac{\delta_L}{S_L}$$

Premixed flames could also burn as laminar flames, and as for all fluid dynamic systems the Reynolds number gives an indication to wether the flow is laminar or turbulent. The most applicable indication is the turbulent Reynolds number defined by the turbulent intensity and the integral length [2].

$$\mathrm{Re}_T = \frac{\rho \cdot l_0 \cdot u'}{\mu}$$

If the turbulent Reynolds number is greater than unity then the flame could be considered turbulent.

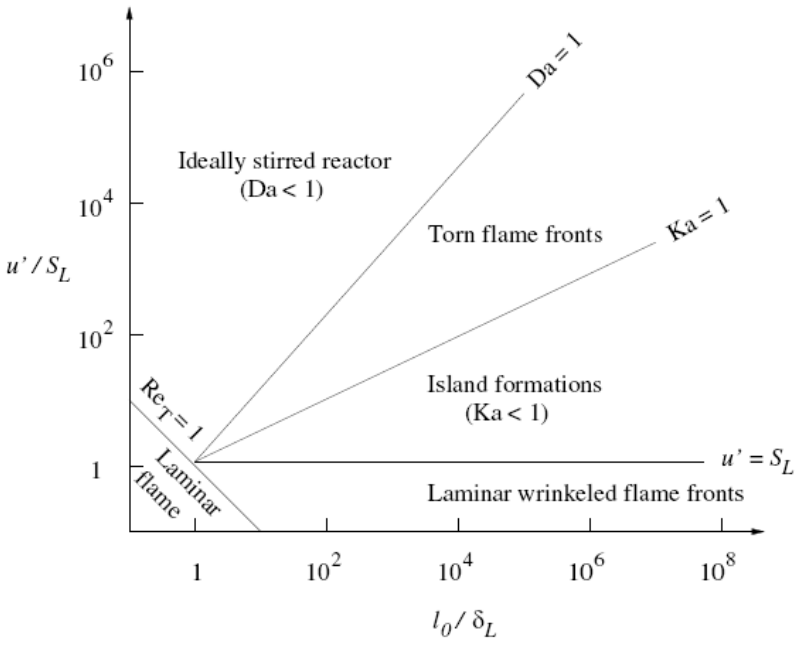

Figure 3.7: Borghi diagram where u' is the turbulent intensity, S_L is the laminar burning velocity, l_0 is the integral length scale and δ_L is the laminar flame thickness. [2].

The flame could be considered the analogy of the ink spot in the water. If there are turbulent eddies larger that the flame thickness in front of the flame it could stretch and wrinkle the flame leading to increased flame area. This is usually the case when the turbulent intensity is fairly low as with $u' < S_L$. In some cases the turbulence could wrinkle the flame so much that different parts of the flame front create burning islands in front of the flame. Island formation is typical when $l_0 > \delta_L$, $u' > S_L$, and $\tau_\eta > \tau_c$. Even though $u' > S_L$, u' is only in the range of medium intensity. If the intensity is even higher and the Kolmogorov length is shorter than the flame thickness, the turbulence could influence the flame just like the ink spot is influenced in example b) in figure 3.6. The flame front could be stretched and expanded by the Kolmogorov scale turbulence, and the inner flame structure could be altered. This regime of the turbulent combustion could lead to local quenching of the flame front since the regime is characterized by a longer chemical time than the Kolmogorov time but lower than the integral time. And it's actually when $\eta < \delta_L$ that the flame could be considered highly turbulent, because the opposite case could be considered only as a deformation of a laminar flame. If the intensity is further increased so that the chemical time is larger than the integral time the regime has difficulties defining the flame since it's highly influenced by the largest eddies. This regime is often referred to as a well stirred reactor.

There are several different regimes of turbulent combustion, and the boundaries between them are hard to describe, but it quit easily illustrated in the Borghi diagram. The Borghi diagram is shown in figure 3.7. It's easy to see

the boundaries between the regimes. The boundaries are given by the Karlovitz number and the Damköhler number.

$$Ka = \frac{\tau_c}{\tau_\eta} = \frac{\delta_L \cdot u'(\eta)}{S_L \cdot \eta}$$

and

$$Da = \frac{\tau_{l_0}}{\tau_c} = \frac{S_L \cdot l_0}{\delta_L \cdot u'(l_0)}$$

3.4 Detonations

This chapter will give a brief introduction to detonation of gases. First is a short description of detonation waves, followed by a description of DDT with reference to experimental research. At the end of this section is a brief reference to different detonation criteria and some special cases of detonations.

Detonation is a term often misunderstood, and often referred to as when a high explosive explodes or when a gas cloud burns fast. As will be described, a detonation can occur in gases, but a gas explosion does not have to detonate.

To describe a detonation, lets start with what it's not. Earlier discussed premixed flames are deflagrations and are subsonic. Deflagrations have the possibility to send information ahead of the flame. Detonations are super sonic and sends no information in front of it. The detonation theory of Chapman and Jouguet (CJ) is a one dimensional consideration satisfying the Rayleigh line and the Hugoniot curve. The CJ theory describes one wave, but Zeldovich, von Neumann and Döring (ZND) proposed that a detonation wave is a coupling between a shock and a reaction zone. The shock wave has heated the gas in front of the flame which makes it auto ignite, [8, 27]. The coupling between the shock and the flame is usually not static, the distance between them can be seen as a moving rubber band, which stretch and contract all the time. A sketch of a one dimensional (ZND) detonation is given in figure 3.8.

Detonations are highly three dimensional phenomena, waves expand spherically and interact with each other. In a detonation there are also transverse waves which makes the detonation front bubble like. The point where two waves meet is called a triple point, and the trajectory of triple points make up a cellular structure. A sketch of the structure is given in figure 3.9. The detonation cell size is often used as a "length scale" charaterizing the detonability of the gas mixture. Each mixture of gas has a cell size. The cell size is not a specific size but more of a approximate size, since it is dependent on many factors such as temperature, pressure and concentration [9]. In general, larger cell sizes indicates higher resistance towards detonations [2]. Information about cell sizes can be found in the detonation database [23]

Some selected cell sizes are given in figure 3.10, [10].

3.4.1 Deflagration to detonation transition

> DDT is a basic combustion problem that has been called one of the major unsolved problems in theoretical combustion theory. Elaine S. Oran and Vadim N. Gamezo [11]

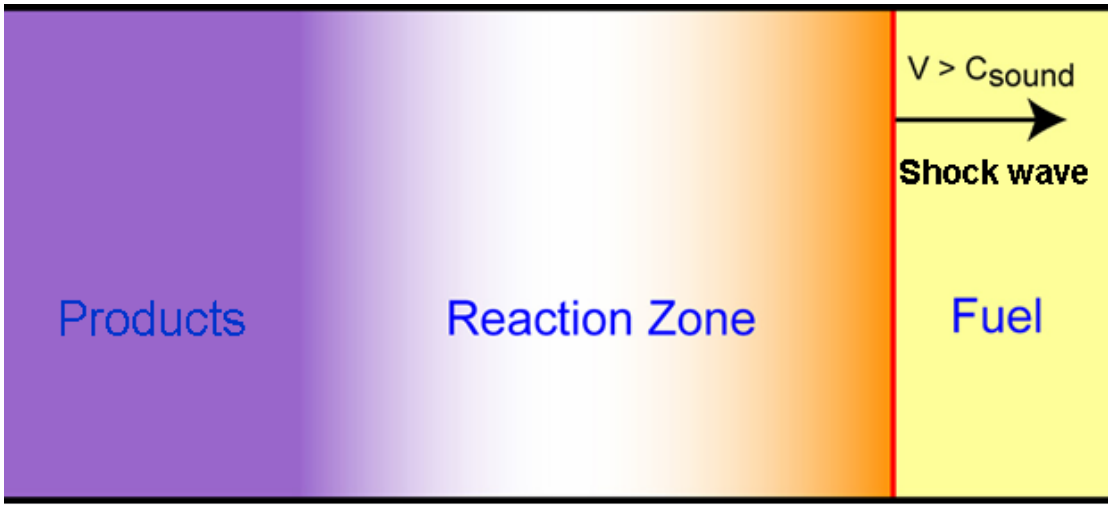

Figure 3.8: A sketch of how the reaction zone follows the shock wave. [26]

DDT can be thought of as an "explosion in the explosion" [12 as referred to in [2]] or "local explosion". The transition from a subsonic combustion wave to a super sonic one is proposed to be due to one of two methods. One method is caused by shock waves which heat up the gas and causing it to self ignite. The other method is transition caused by instabilities in the flame, which could make pockets of reactants. These pockets could in turn explode in the explosion, [13 as referred to in [2]]. Lee et. al. [14 as referred to in [2]] proposed that DDT happens in a gradient of induction time (τ_c). The mechanism is called Shock Wave Amplification by Coherent Energy Release (SWACER). This can be though of as a gradient of reactivity, where one area has a low induction time and has short time before reaction takes place. The neighboring area has a little bit longer induction time and so on. When the first area explodes it sends out a shock wave. When the shock wave passes the neighboring area it increases the temperature and pressure and it explodes, the explosion fuels the shock wave which passes through the next area and compresses and heats that area. The reaction wave will move with a speed D, [11].

$$D = \left(\frac{\partial \tau_c}{\partial x} \right)^{-1}$$

This speed must be higher than the laminar flame speed but there is in general no upper limit regarding the speed of the reaction wave. It is not even limited by the speed of light [11]. This mechanism goes on until it detonates, and the reaction zone follows the shock wave [2].

DDT can happen in many different cases, and at the moment there are no exact method of predicting DDT. Pipes with obstacles are well known to initiate DDT. Obstacles are also know to both quench and reinitialize detonations [15]. DDT can happen in smooth pipes too, it's usually a matter of the length and diameter of the pipe.

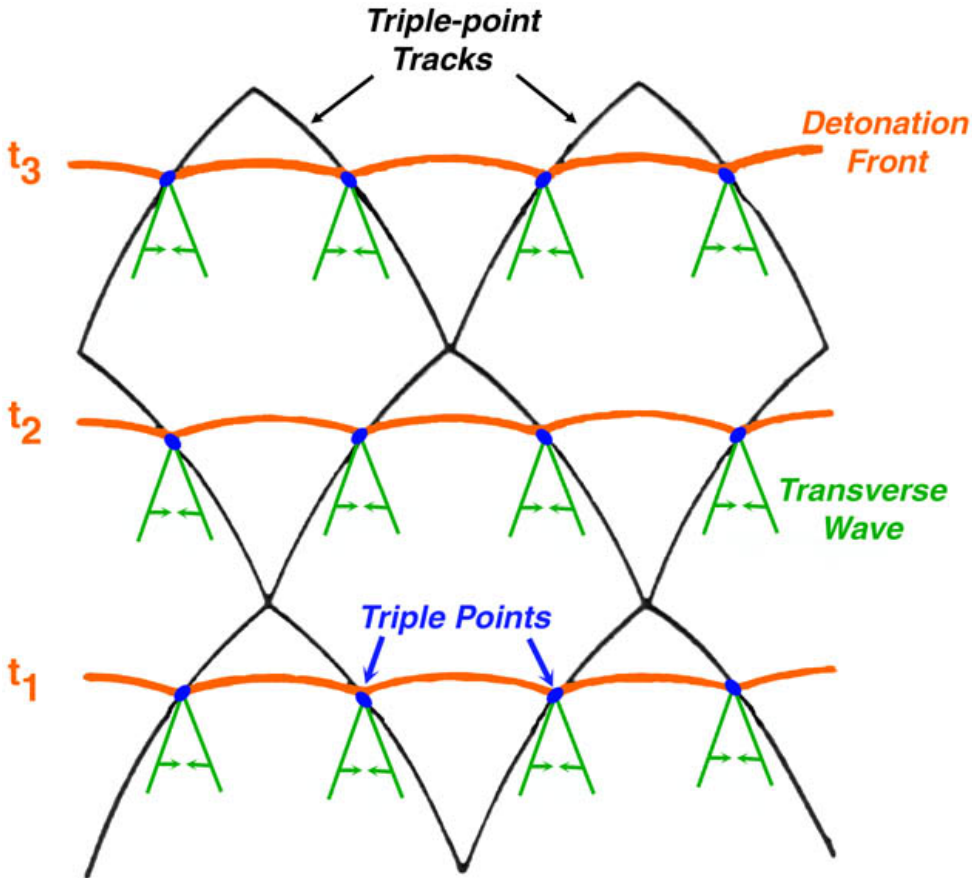

Figure 3.9: A sketch showing how the trajectory of triple point make up a cell structure. [26].

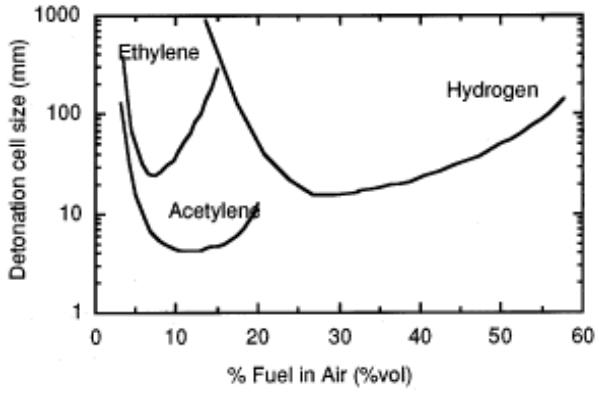

Figure 3.10: Cell sizes for hydrogen, ethylene and acetylene for different concentrations. [10]

Experimental studies of DDT

In a pipe with a single obstacle there are basically three different cases of detonation initiation and DDT. One is DDT caused by the accelerated flame, an other is initiation of detonation caused by reflected shock waves and the last is DDT in a turbulent jet through the obstacle. Presented below is three different experimental researches addressing the topic.

Urtiew and Oppenheim did several experiments with DDT in an explosive gas [27,12]. They observed that the transition could occur several places in a system of flame propagation in a pipe. There is a run-up distance before DDT occur, but the mode of DDT could vary. The mechanisms of the different transition modes depend highly on the wave structure in the system. The four different modes where transition from deflagration to detonation could occur is:

1. Between the flame and the shock wave. See figure 3.11 (a).
2. In the flame front. See figure 3.11 (b).
3. At the shock. See figure 3.11 (c).
4. At contact discontinuity. See figure 3.11 (d).

Steen and Schampel [16 as referred to in [2]] has given a linear correlation between the pipe diameter and the run-up distance (the distance from ignition until DDT occur). This indicates that for a given mixture the ratio between pipe diameter and run-up distance is constant. He [17as referred to in [2]] has also proposed that DDT happens at conditions above certain critical integral lengths and critical turbulent intensity.

It is impossible to exactly reproduce a transition, quoting Kuo. K. K. (1986):

> Since the generation of any particular pattern depends on some minute inhomogeneities in its development, the process of transition to detonation is nonreproducible in its detailed sequence of events. [27].

Brown and Thomas (1999) [28] did experiments with a shock tube and a schlieren photography. The experiments started with sending a shock wave through a section of inert gas to stabilize the shock before it propagated through an explosive mixture of diluted propane-oxygen or ethylene-oxygen mixture. The end of the experimental channel was closed. The setup is described in figure 3.12.

When the shock wave hit the end plate and reflected, they observed an initiation of detonation in some experiments. The mechanism of the initiation was that the shock wave compressed and heated the gas and when it reflected of the end plate it was further compressed. This compression created gradients of reactivity from the wall, and the gas mixture auto ignited and continued as a detonation. The results are shown in figure 3.13 and showing three different experiments. Experiment (a) shows a mixture of $C_2H_4 + 3O_2 + 96Ar$ and a shock strength of Mach 2.65, (b) shows mixture of $C_2H_4 + 3O_2 + 12Ar$ and shock strength Mach 2.64, (c) shows mixture of $C_2H_4 + 3O_2 + 12N_2$ and shock strength Mach 3.11. Experiments (b) and (c) shows a initiation of detonation, while (a) does not detonate.

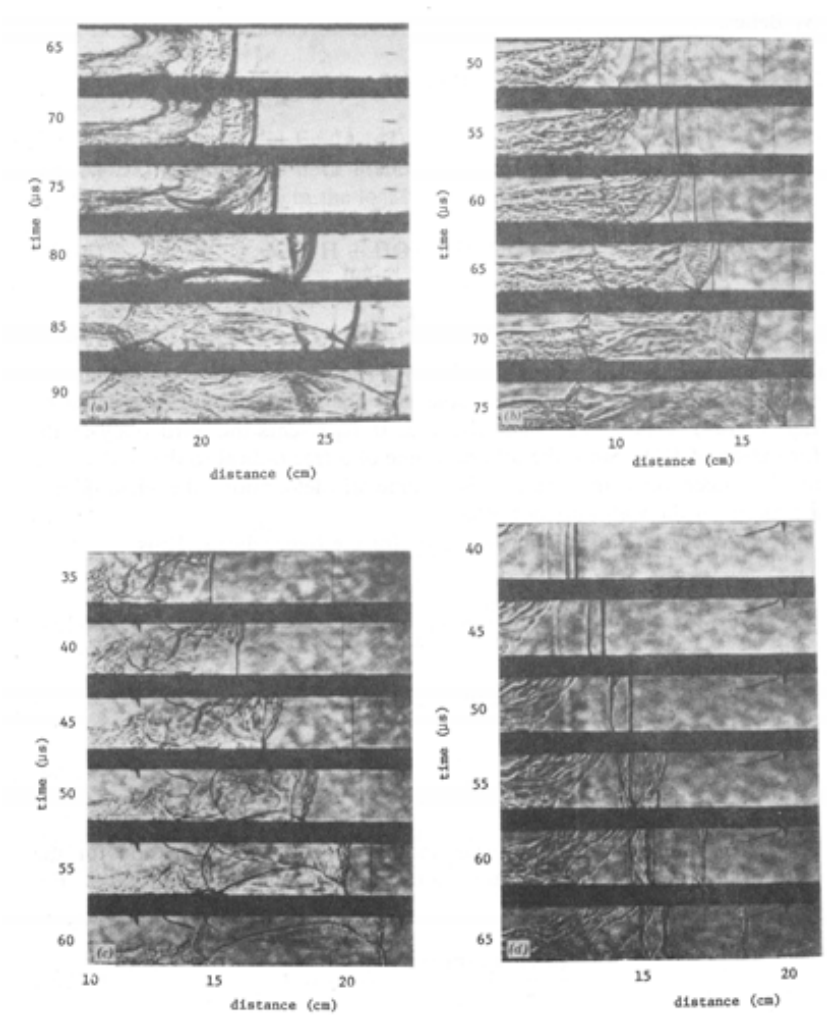

Figure 3.11: The esperiments done by Urtiew and Oppenheim with $2H_2 + O_2$. (a) transition between the shock and the flame. (b) transition in the flame front. (c) transition at the shock. (d) transition at the contact discontinuity. [12].

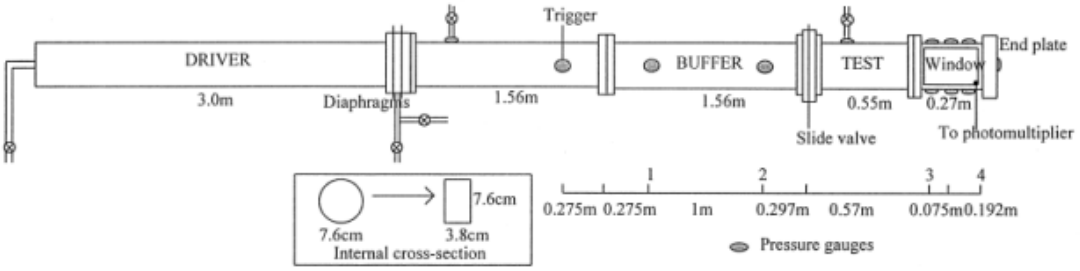

Figure 3.12: The setup of Brown and Thomas. [28].

There has also been observed detonation initiation or DDT in turbulent jets. Moen [19] explains that several experiments have shown that detonation could be initialized in a turbulent jet of a fuel-air mixture. Moen refers to different large scale experiments with different combustible gases. The experimental results clearly shows that a turbulent jet fire from a tube into an unconfined volume of combustible gas has the possibility of detonation initiation. Moen also proposed a connection between the ratio of critical tube diameter (approx. thirteen times the cell size) to tube diameter and the initial jet velocity, with a limit between experiments with detonation and experiments without detonation. For details about the relation between jet velocity and diameters, see Moen (1993) [19].

3.4.2 Detonation criteria

There is no full understanding of the mechanism of DDT. If one wants to initiate DDT, there are certain criteria that should be fulfilled. There has not been observed DDT of fuel-air mixtures in unconfined geometries, there is always a confinement present of some sort [15].

Lee et. al. experienced that detonations occurred in pipes when the cell size of the mixture was smaller than the pipe diameter [18 as referred to in [2]]. For obstacle filled closed pipes Peraldi et. al. [20 as referred to in [2]] has proposed that the diameter of the obstacles has to be larger than the cell size.

There is also a regime of detonations known as quasi detonations [21]. Teodorczyk [15] did experiments in obstacle filled square channels and observed an overall detonation velocity as low as 50% of the CJ velocity. Detailed investigation reveal that the regime is a series of detonations which decouples around the obstacles. But reflecting shock waves reinitialize the detonation again behind the obstacle.

There are a possibility that DDT might occur in the experiments done in conjunction with this report. As explained in the next part the flame will form a funnel of reactants in the middle of the pipe. When a shock wave is reflected at the ignition end of the pipe it passes through the flame and compresses and heats the gas in front of the flame. This will make a gradient of induction time, which is what Lee et. al. proposed to be a location where DDT might happen. There is also a possibility that the mechanism of reflected shock wave initiation could start a detonation at the obstacle in the experiments. Detonation initiation in

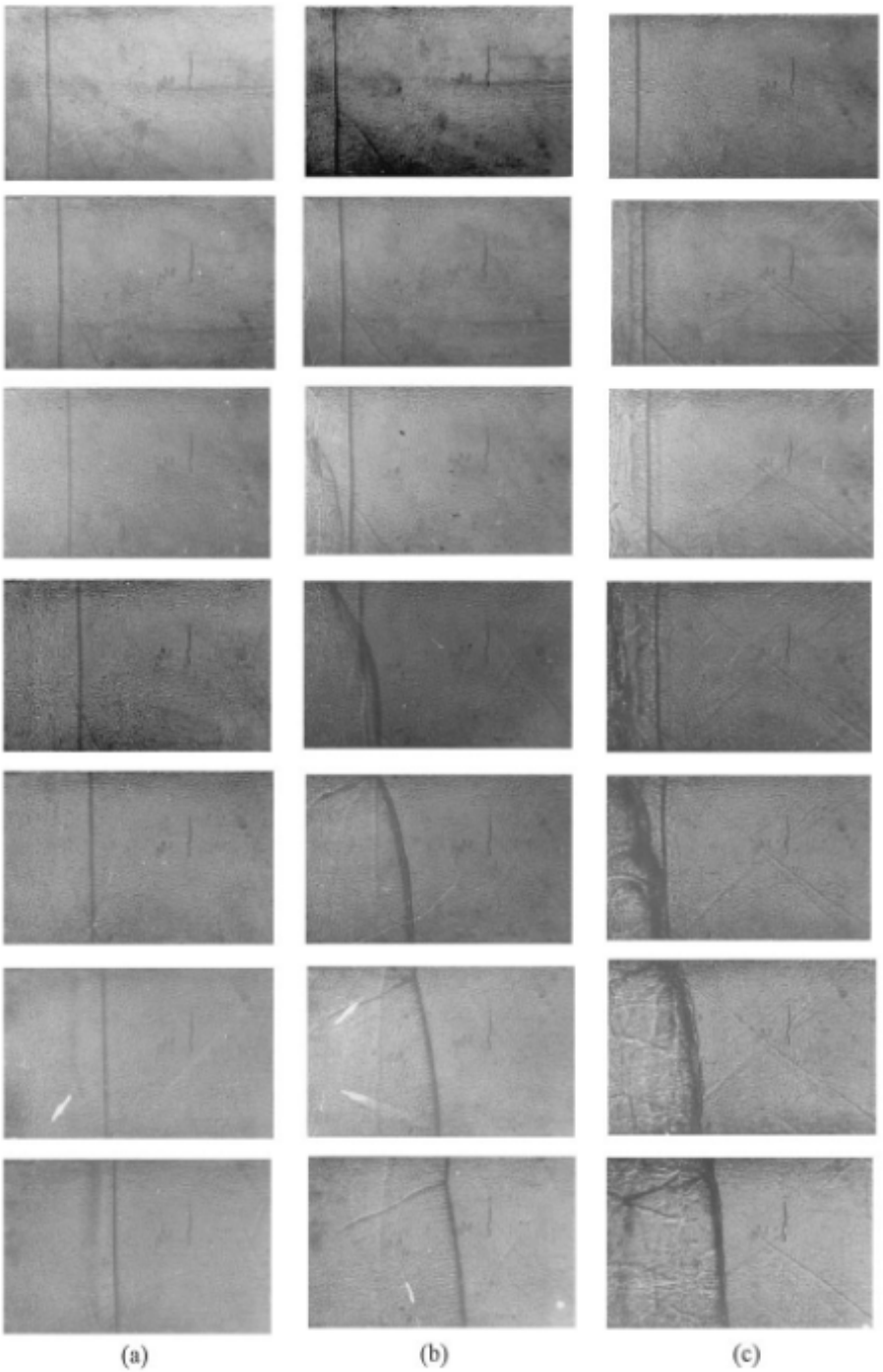

Figure 3.13: Eperiment (a) shows a mixture of $C_2H_4 + 3O_2 + 96Ar$ and a shock strength of Mach 2.65, (b) shows mixture of $C_2H_4 + 3O_2 + 12Ar$ and shock strength Mach 2.64, (c) shows mixture of $C_2H_4 + 3O_2 + 12N_2$ and shock strength Mach 3.11. Initial pressure 0.0526 atm. and 10 μsec. frame spacing. [28].

a jet formed at the obstacle is also a possible case where detonation could be initiated.

Chapter 4

Experiments

Flame propagation in a circular pipe has been studied for this report. The motivational background of the experiments with hydrogen explosions in a pipe with a single obstruction, was earlier work done by Knudsen, Vågsæther and Bjerketvedt, [1-2]. Vågsæther and Bjerketvedt [1] simulated an explosion in a pipe with hydrogen-air mixture, The pipe had a single obstacle. The setup was the same as the experiments done by Knudsen [2]. The simulations calculated that the flame inverted before it reached the obstacle. The experiments done by Kundsen [2], could not determine if the flame inverted before the obstacle. The background for the experiments in this report was to film the first part of a similar pipe, and investigated inversions of the flame, and find out what causes the inversion.

4.1 The experimental setup

The experiments were performed at the Telemark University College (TUC) in Porsgrunn Norway, and a sketch of the setup is given in figure 4.1

The setup was a transparent tube with ignition in a closed end and an orifice plate, with a 30mm opening (obstacle), at the open end before a steel tail pipe. Three pressure transducers were placed on the pipe before and after the obstacle and the flame propagation were filmed with a high speed camera. The transparent pipe (see 4.2) was made of Lexan with steel flanges in both ends. The total length of the pipe was 1000 mm and the length of the transparent part was 860 mm. The inner diameter of the pipe was 97 mm.

The steel tail pipe had inner diameter of 105 mm and a length of 300 mm. The end of the steel pipe was open the atmosphere. The ignition system was a high voltage spark generated by a Trafo Union Siemens ignition unit model ZM 20/10. The ignition spark was placed at the closed end of the Lexan pipe and generated 10 kV and 20 mA. The spark plug had metal wires placed 2 mm apart. The gas inlet and ignition setup is shown in 4.3. The inlet pipe had an inner diameter of 17 mm, and the last 12 mm before it entered the Lexan pipe had a diameter of 22 mm. Ignition spark plug was placed 50 mm inside the inlet pipe. Gas inlet could be turned on or off with a ball valve.

The obstacle was an orifice plate with a 30 mm diameter opening in the center. This orifice plate will also be called the obstacle. The thickness of the

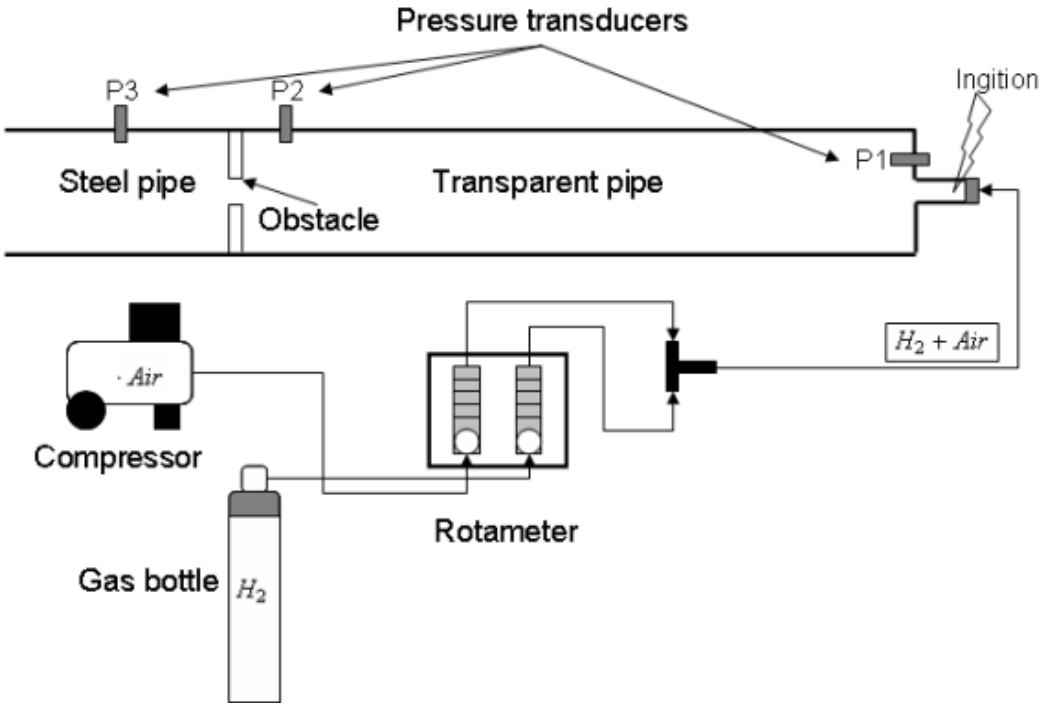

Figure 4.1: Sketch of the experimental setup.

Figure 4.2: Showing the transparent Lexan pipe, steel flanges and steel tail pipe. The obstacle is placed between the tail pipe and the flange.

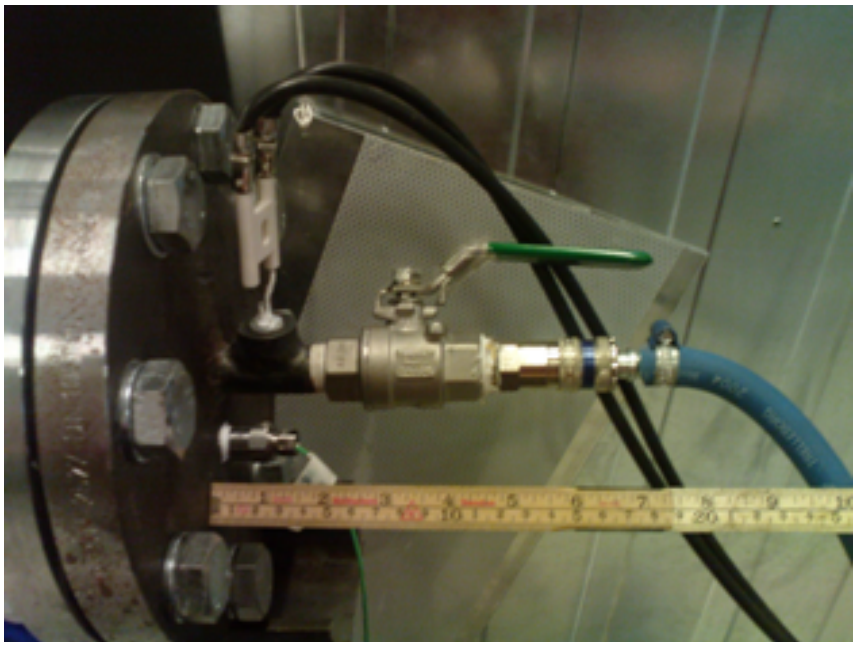

Figure 4.3: This picture shows the inlet to the pipe and the ball valve. Also shown is the ingnition and one pressure transduser.

orifice plate was 18 mm.

The pipe was tilted downwards at 7.2^0, with the outlet as the lowest end.

The pressure transducers was Kistler 7001 quartz high temperature pressure sensors and the amplifier was Kistler 5011 charge amplifier. One sensor was mounted at the closed end of the pipe normal to the axial direction. One sensor was mounted 40 mm before the obstacle (960 mm from the closed end) parallel to the axial direction, and the last pressure sensor was mounted 150 mm behind the obstacle (1172 mm from the closed end). The pressure transducers are shown in figure 4.3 and figure 4.4.

Air was supplied from an air compressor at 4 bar pressure. Air pressure was reduced in a pressure regulator valve to 1 bar. Hydrogen was supplied from a hydrogen gas bottle with 1.5 bar working pressure.

The data was logged by Sigma Series Transient Oscilloscope. It logged 1e6 point in 0.5 sec. The whole system was triggered by a Quantum 9500 plus Series Pulse Generator. The pulse generator triggered the camera and the ignition, but also the oscilloscope.

4.2 Experimental procedure

Every experiment was conducted in the same matter, but done at two different days. As the earlier setup was installed the procedure for each experiment was as following. Hydrogen bottle was opened and correct pressure checked. Air pressure was also checked and H_2 and air flow through the rotameters was adjusted accordingly to desired concentration. The pipe was filled for more

Figure 4.4: The tailpipe, obstacle, pressure transducers number 1 and 2 and outlet of the pipe.

than two minutes, corresponding to filling the pipe at least two times. After at least two minutes the hydrogen bottle was closed and the inlet ball valve was closed. The system was triggered, first triggering the high speed camera and the oscilloscope at time zero. There was a very short and varying pretriggering of the high speed camera but it didn't influence the result since the time zero of the movie corresponds to the time zero of the rest of the system. The oscilloscope also had 0.05 sec. pretriggering. The ignition was triggered at time zero, but due to 50Hz oscillations in the electricity supply from the power grid the ignition could vary with 20 ms. After the experiment, the inlet ball valve was opened so the pipe could be flushed with air until next experiment. The pressure signals was recorded by the oscilloscope and saved after each experiment. The high speed film was cut to only include the flame and saved on the computer. The reason for the cutting was to reduce the size of the files.

The different experiment are given in table 4.1.

The pressure results was combined to one file with different channels and correct amplification and time array was applied. The high speed films was saved on a computer.

The accuracy of the experiments were considered mainly to dependant on the Rotameter settings and the calibration of them. It was assumed that an error of 1 percent in the Rotameter settings was likely the highest error in the experiments. If both the air flow Rotameter and the H_2 Rotameter was 1 percent wrong, the error in the H_2 concentration was approximately 0.5 percent. There was likely some error in the calibration of the flow meters, but the experiments were conducted mostly with H_2 Rotameter settings in the middle of

Experiment	Air flow [l/min]	H_2 flow [l/min]	H_2 conc. [%]
1	10.90	2.73	20
2	10.90	2.73	20
3	10.90	3.63	25
4	10.90	3.63	25
5	10.90	3.63	25
6	10.90	4.58	30
7	10.90	3.63	25
8	10.90	4.58	30
9	10.90	4.58	30
10	10.90	5.87	35
11	10.90	5.87	35
12	10.90	7.26	40
13	10.90	7.26	40
14	7.31	7.31	50
15	7.31	7.31	50

Table 4.1: Experimental matrix

the calibrated region. Air flow Rotameter was also calibrated for the 10.9 l/min setting twice.

4.3 Flame propagation in the pipe.

The experimental setup had a transparent pipe with ignition on the right closed end. The gas used for the experiments was hydrogen and air premixed before the pipe. When ignited, the flame propagated from right to left. The flame front encountered inversion when it propagated inside the pipe. Inversion of a flame front is defined as when the center of the flame front moves in the opposite direction of the rest of the flame front. Inversion will create a funnel like shape of the flame front and increase the flame area. One goal of the experiments was to identify inversions of the flame and compare with CFD simulations of pressure wave interaction with flames.
The flame propagation in the pipe will be influenced by many factors, and the goal of this study is to identify some influencing factors. A high speed camera was used to film the flame propagation, and the films has been analyzed using MATLAB to extract the flame front in the top, bottom and center of the pipe, see figure 4.5.

The method of extracting the flame position was based upon finding the position of step changes in a gray scale picture. This was done for every frame of the film. The level of the step changes was slightly different from film to film, but was between 20 and 35. Due to noise in the films, mostly glowing particles, the extraction method gave noisy results as well. The noise was most evident in the beginning and end of the pipe.

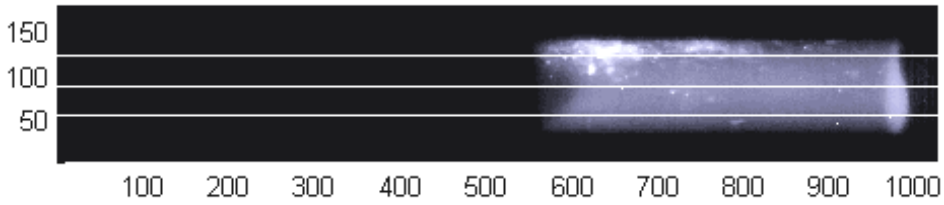

Figure 4.5: Flame position was extracted at the top, bottom and center of the pipe. White stripes indicate the position of extraction.

4.3.1 Flame positions

For this study, three experiments has been analyzed. One experiments with 30% hydrogen concentration and two with 35%. These were the best experiments to analyze, due to less noise than other experiments.

Figure 4.6 (30% H_2) shows that the flame encountered inversion after 0.11 seconds, the center part of the flame front moved further backwards than the top and bottom part of the flame front. There were several other countermarches of the flame front later, but due to noise of the film it was not clear to see if it was inversions or if the whole flame front moves backwards. Figure 4.7 (35% H_2) shows that it is hard to tell if the flame front inverted, or if it stopped and the flame front became flat and then it propagated left again. The figure also shows that the flame had a bubble like front approximately 2/3 down the pipe.

4.3.2 Propagation frame by frame

By selecting frames from the films it was possible to show how the flame stopped moved backwards or even inverted. The frames are not equidistant in time but rather selected to show to phenomena of halted propagation and inversion. In frame 3, 4 and 5, figure 4.8, it is clear that the flame moved backwards and inverted. Again at frame 8 and 9 it's clear that the flame almost stopped, but it is hard to see from the frames if the flame front inverted. The frames shows that the flame front was wrinkled.

Analyzing experiments with 35% H_2 the flame also halted, but it was harder to see if it inverted, see 4.9. Frame 2, 3 and 4 showed the flame moving backwards, but frame 4 and 5 has darker areas in the center, indicating a possible inversion. Frame 5 had a "tip" in the center also, this could be because of 3 dimensional flame front and the flame propagated differently for each cylindrical angle of the pipe. Frame 6, 7 and 8 shows that the flame propagated again and also formed a semi spherical flame front (frame 8), before it halted again (frame 9 and 10).

An other experiment with 35% H_2 showed clearer that the flame front inverted right before the obstacle at the left end of the film. Frame 9 and 10 in figure 4.10 shows that the flame got a funnel like shape before the obstacle. In this series of frames it was clear that the flame front was wrinkled, and has clearly 3D characteristics. From a 2D picture it was hard to determine how the 3D shape of the flame front actually was.

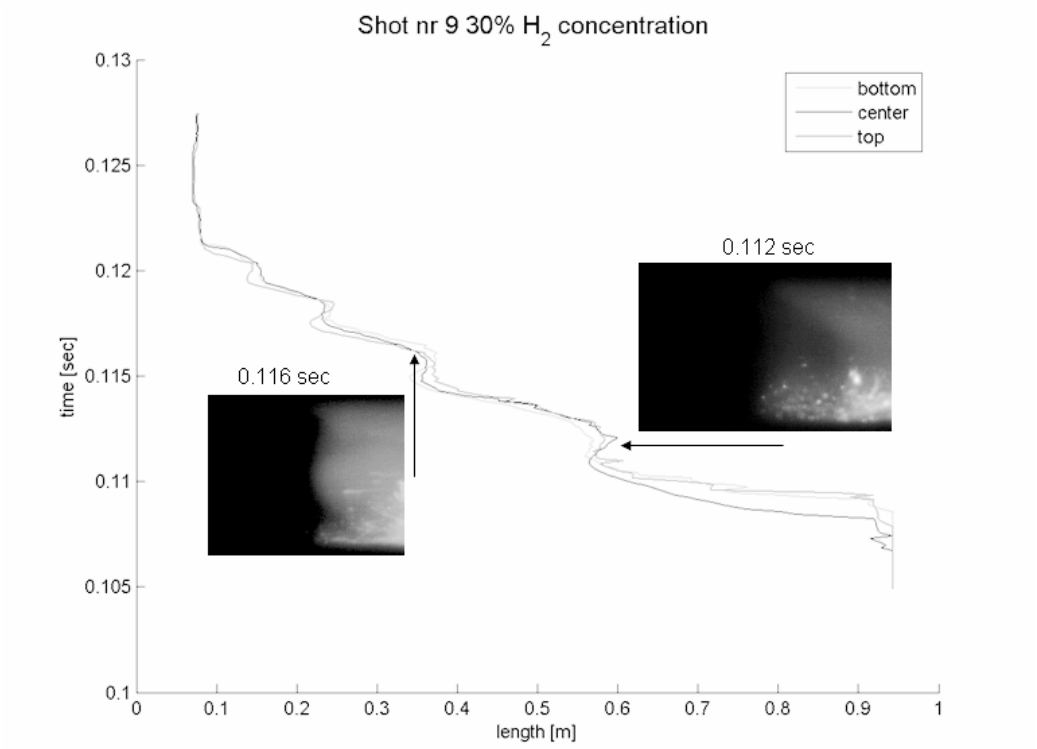

Figure 4.6: The flame position extracted from the film. The flame encounters inversion approximately halfway through the pipe.

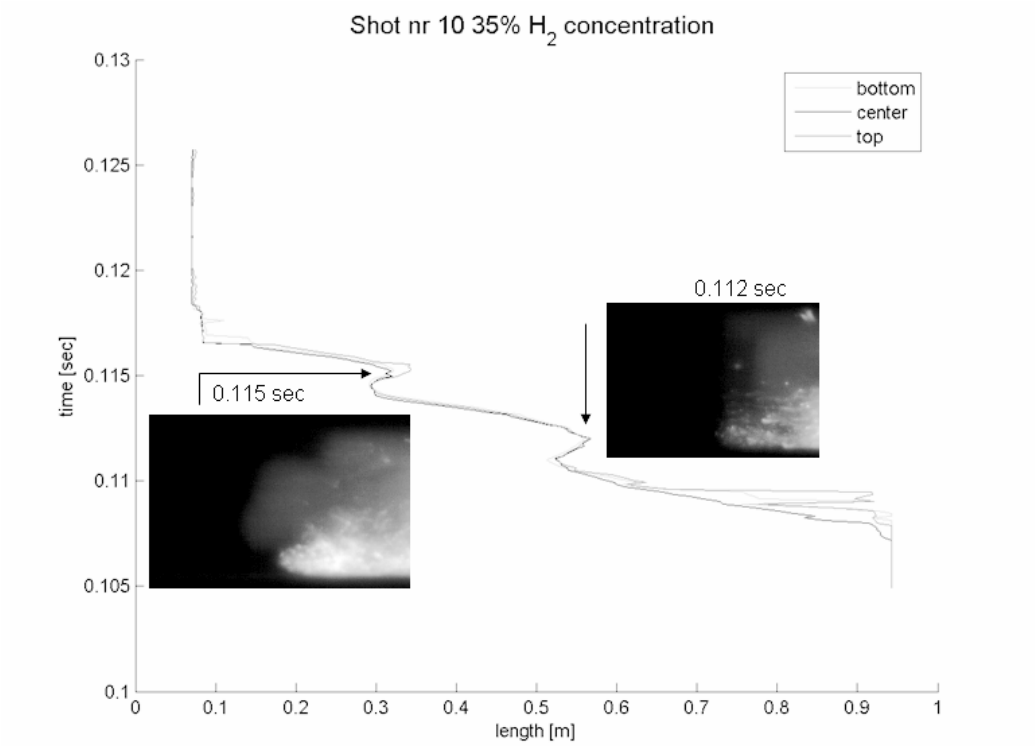

Figure 4.7: The flame position extracted from the film. The flame had a bubble like front approximately 2/3 down the pipe.

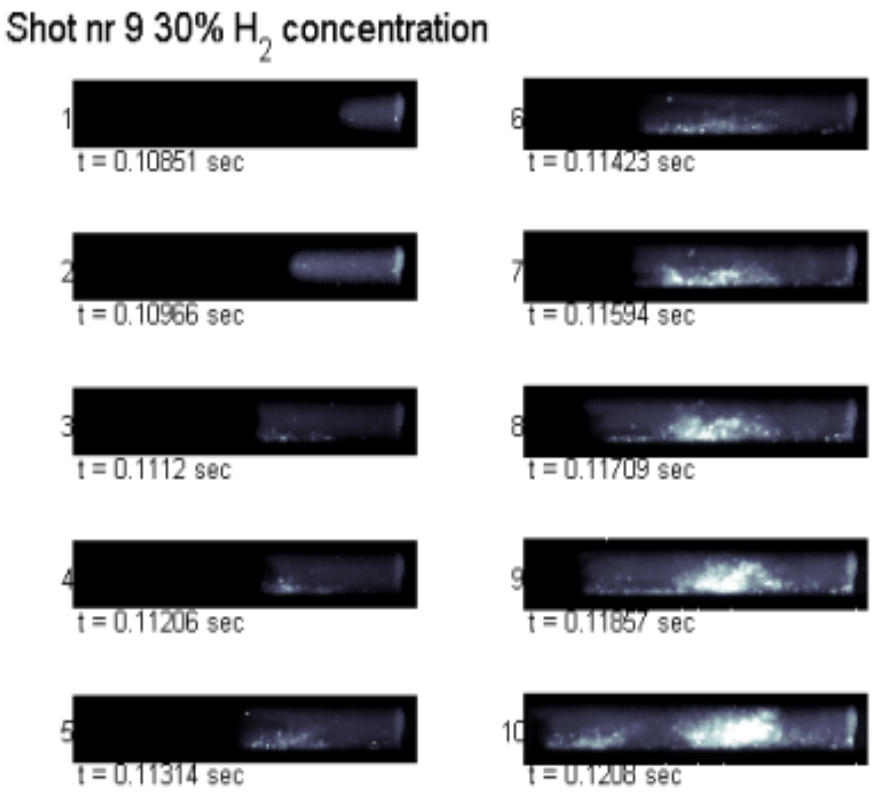

Figure 4.8: Flame propagation shown frame by frame. It was clear that the flame inverted (frame 2, 3 and 4). The flame almost halts later (frame 8 and 9).

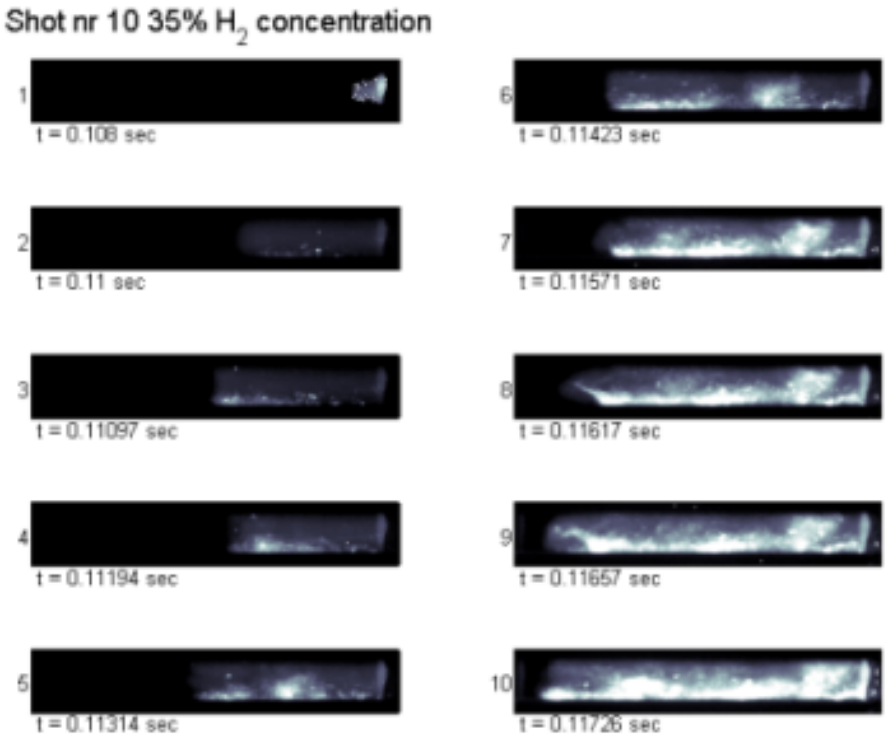

Figure 4.9: For 35% H_2 it was harder to see if the flame inverted. It halted and countermarched, but inversion is harder to see. Frame 4 and 5 showed darker areas in the center, but also a longer "tip" in front.

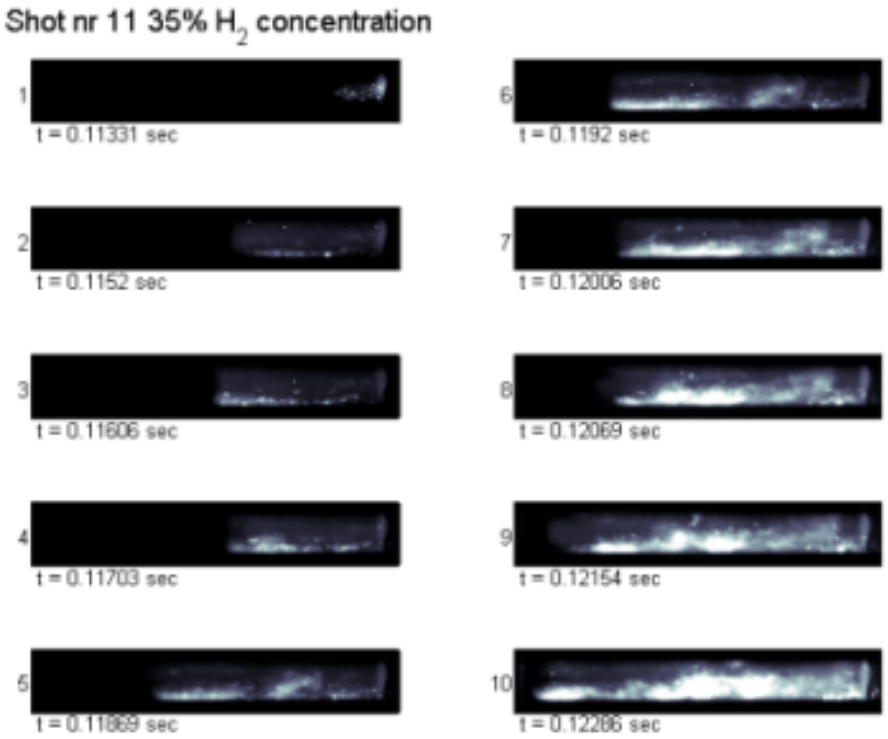

Figure 4.10: The last frames indicates that the flame inverted.

Shock waves could be seen in some of high speed films, but propagating shock waves can not be visualized on paper. Experiment 13 with 40% hydrogen showed a shock wave propagating through the flame from behind when the flame was inverted. The shock wave propagating through the flame also reflected off the flame, but didn't influence the shape very much

4.3.3 Pressure records

The pressure was recorded from the experiments. Three pressure senors were mounted on the pipe. One sensor (sensor 1) were mounted on the closed end where the gas was ignited, one sensor (sensor 2) was mounted before the obstacle (orifice plate with 30 mm opening), and the last sensor (sensor 3) was mounted on the middle of the steel tail pipe, see figure 4.1. Three experiments was investigated for this report, one with 30% H_2, one with 35% H_2 and one with 40% H_2. The pressure records were filtered using a lowpass filter with sampling time of 10e-5 sec. and a filter time of 3e-5 sec. Comparison of pressure records and film was investigated to find connections between pressure waves and flame front behavior. By scaling and transposing figure 4.6 and plotting together with the pressure records of the same experiment, see figure 4.11. The pressure waves hit the obstacle and reflected back towards the flame, after the pressure wave was reflected the flame halted and even countermarched. This indicated that the pressure waves caused the stopping and possible also the inversion of the flame. The pressure waves had shape similar to acoustic waves rather than shock waves.

It was also evident from other experiments that there was a relation between pressure waves and halted flame propagation, see figure 4.12. Remember that the vertical axis is both the pressure and a scaled and transposed position of the flame.

4.3.4 Comparison of different experiments

The pressure results from the experiments showed that there was a pressure peak approximately when the flame passed through the obstacle. The 30mm opening forced the gas to form a jet through the obstacle, thereby creating high turbulent intensity and faster burning rate, more energy released resulting in higher pressure. The waves moved back an forth between closed end and obstacle, this phenomena was easily seen in the high speed film of the experiment. The shock waves was not visible with frame by frame visualization. The experiment with 35% H_2 concentration had higher peak pressure than the experiment with 30% H_2 concentration. One other remark was that the highest pressure peak of the 30% H_2 experiment was first recorded on sensor 3 behind the obstacle, then on sensor 2 right before the obstacle and at last on sensor 1 at the closed end. The 35% H_2 experiment had the highest pressure peak recorded on sensor 2 before sensor 1 and sensor 3, but also a reflected pressure wave, possibly reflected from the closed end, recorded on sensor 2 after the peak recorded on sensor 3. This might indicate a high energy release between the closed end and the obstacle, contradicting the 30% H_2 experiment with the highest energy release in or after the obstacle. From the high speed film it was not clear to see if the flame passed through the obstacle before the first of the highest pressure peaks, because the last 70 mm of the pipe was not transparent. Even though it was clear from the

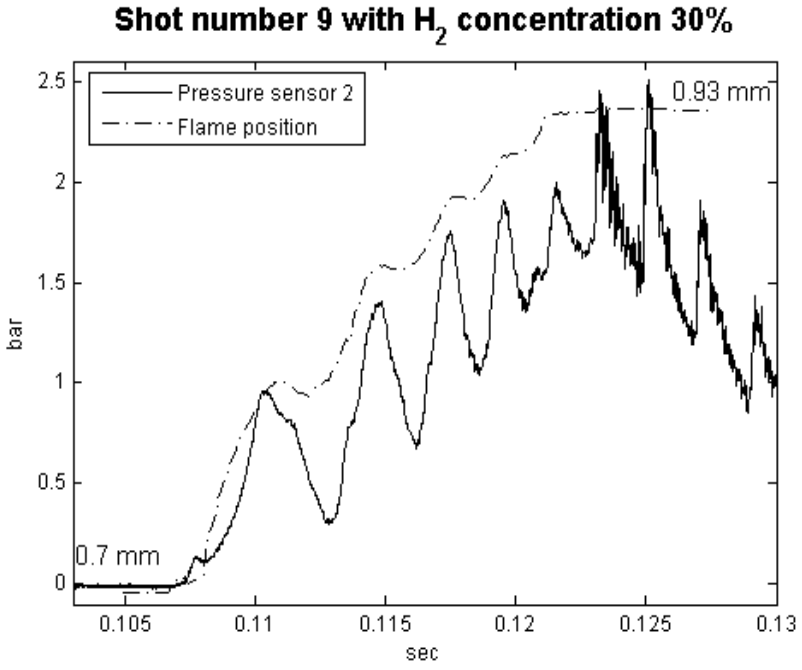

Figure 4.11: Flame position and pressure records from sensor 2. Pressure waves hit the obstacle and reflected back towards the flame. The position is also indicated on this plot to illustrate the link between pressure peak and countermarch.

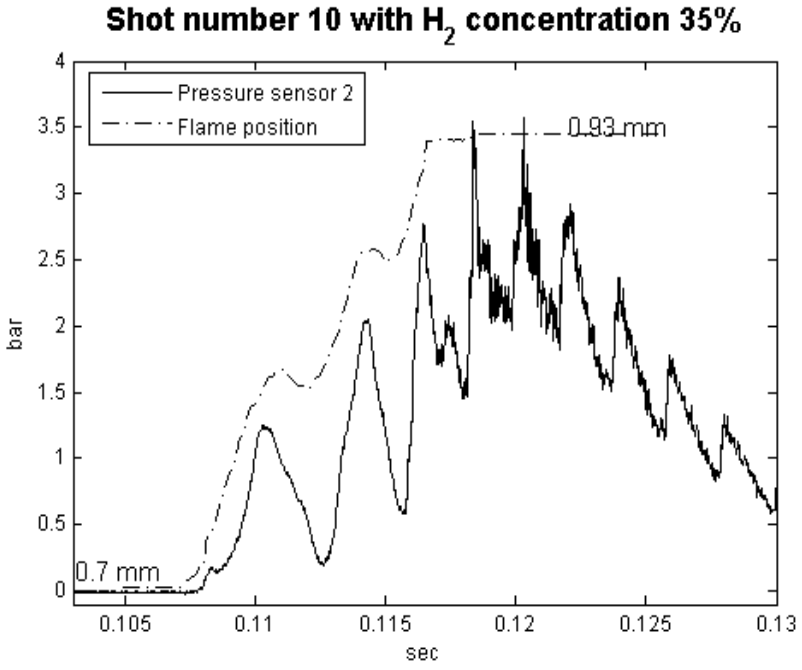

Figure 4.12: Ralation between pressure waves and flame position. The figure shows clearly that there is a conection between pressure peaks and halted propagation of the flame. With earlier figures it is also shown that the flame inverts.

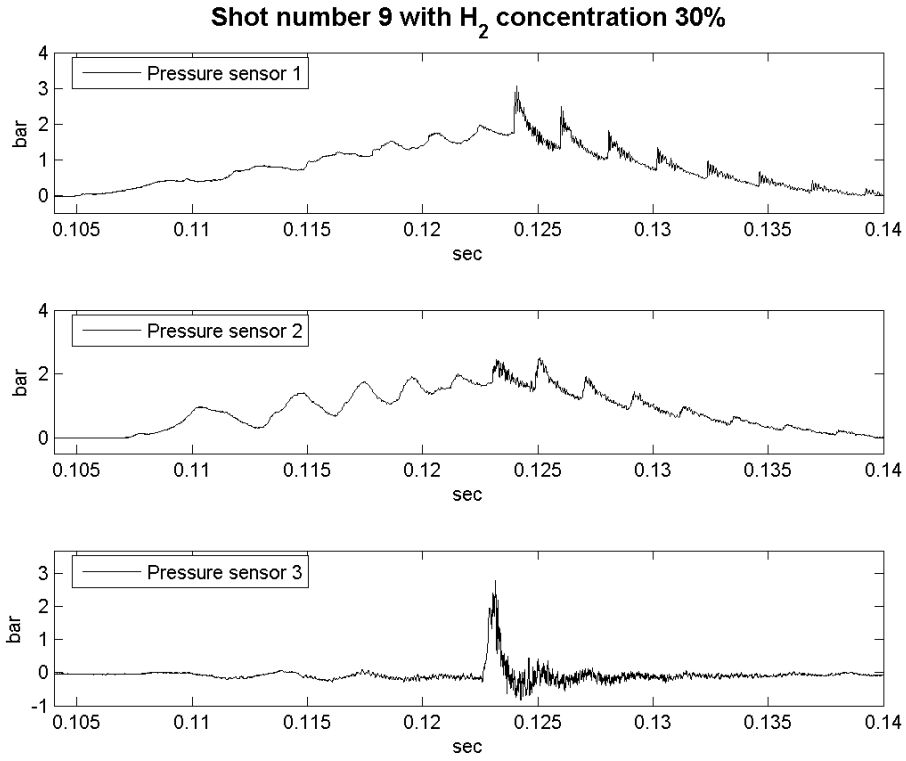

Figure 4.13: Pressure records of 30% H_2 experiment.

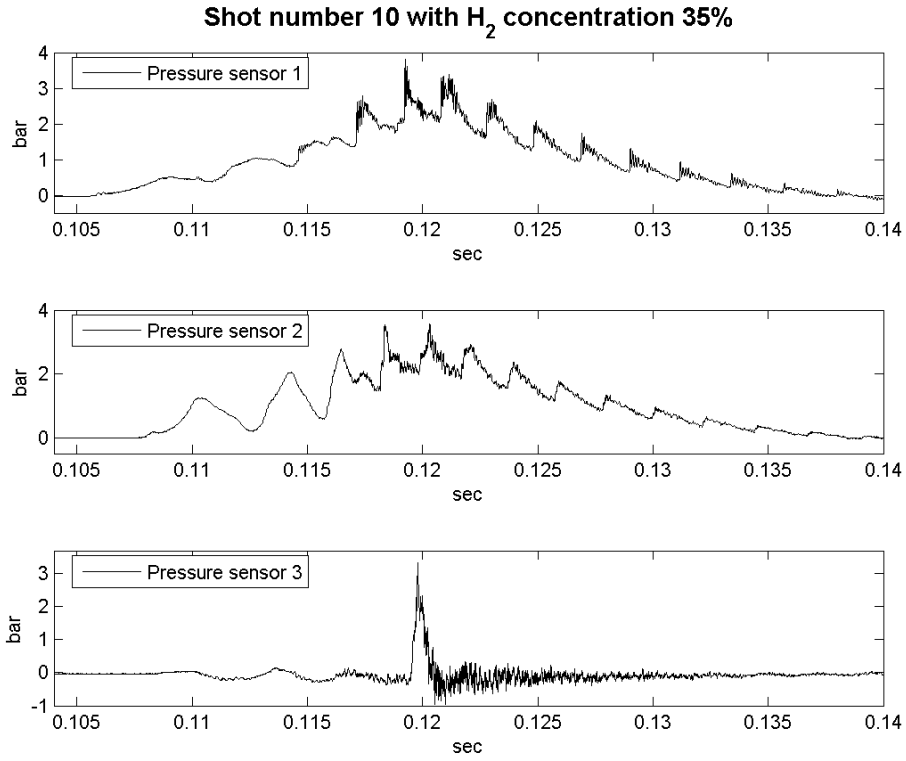

Figure 4.14: pressure records of 35% H_2 experiment.

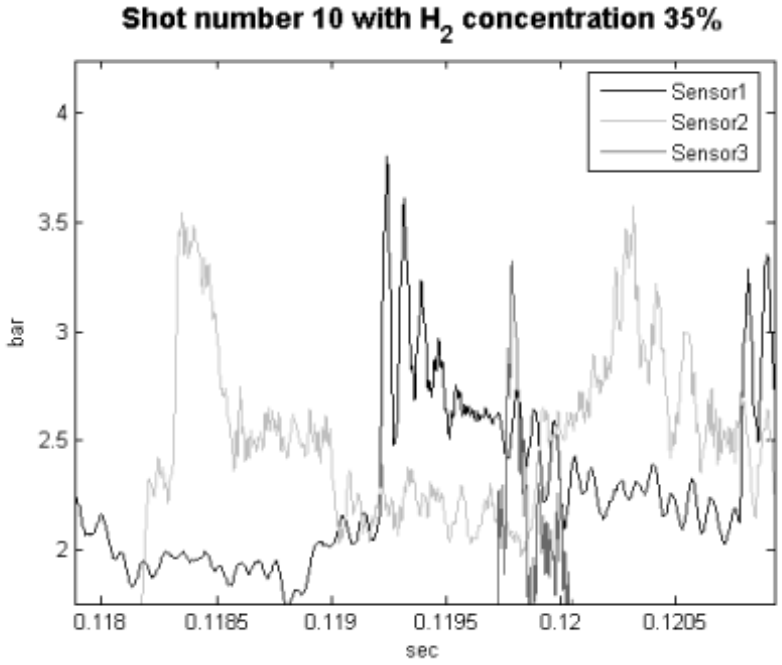

Figure 4.15: Zoomed view of the pressure peaks showed clearly when the pressure waves hit the different sensors.

pressure records that the highest pressure peak was recorded on sensor 1 0.6 ms before it was recorded on sensor 3. A zoomed picture showed the details of the pressure peaks, see figure 4.15. The 40% H_2 experiment had almost the same pressure levels as the 35% H_2 experiment. It seemed to form a shock wave before the flame reached the obstacle, but the order of the pressure peaks were different. First the peak reached sensor 2 then sensor 1 then sensor 2 again before sensor 3 and sensor 1.

4.4 Discussion

The experiments rises some essential questions regarding different topics of flame propagation. Answers to the questions will be proposed but are most certainly up for discussion. To clarify the experiment it's necessary to describe the event history of the experiment from ignition until all gas is burned. In this part only three experiments will be discussed. It's one experiment with 30% H_2 one with 35% H_2 and one with 40% H_2.

4.4.1 Event history of experiment 9 with 30% H_2 concentration

Ignition was established from the spark plug. Not seen in the film but it's likely to assume that the flame expanded spherically until it reached the pipe wall. The burning rate was assumed to decrease when the flame hit the pipe

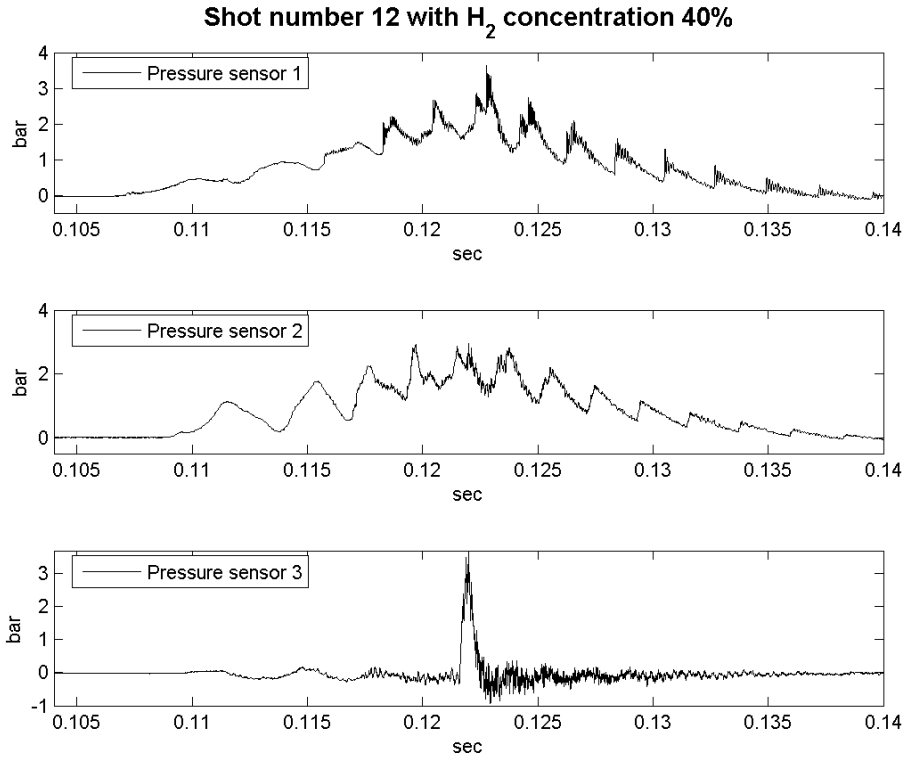

Figure 4.16: Pressure records of 40% H_2 experiment.

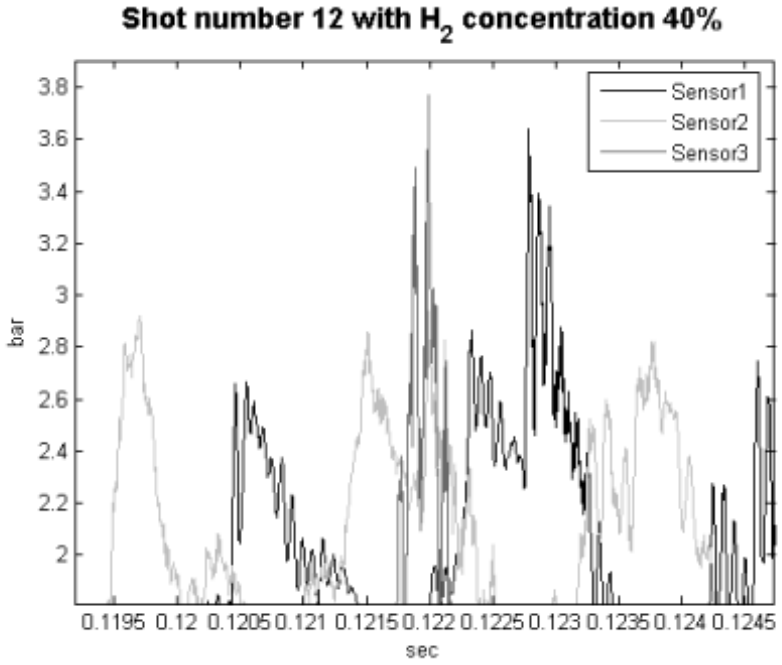

Figure 4.17: Zoomed view of the pressure peaks showed clearly when the pressure waves hit the different sensors.

wall. After that the flame accelerated through the first $\frac{2}{5}$ th. of the pipe. This acceleration might possibly be due to generation of turbulence and increased mixing in the flame. At this point the flame sent pressure wave in front of it towards the obstacle. When the pressure wave was reflected at the obstacle and propagated towards the flame it caused the flame to stop (relative to the pipe) and even invert. This interaction will be discussed later. When the pressure wave passed the flame it started to propagate further towards the obstacle, but with an funnel of unburned gas in the middle of the pipe. This funnel was visible in the film, but three dimensional flames are hard to explicitly interpret in two dimensional pictures, see figure 4.18.

After a while the funnel collapsed, but at the same time a new pressure

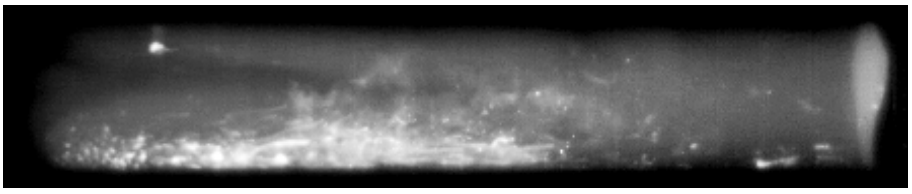

Figure 4.18: It can be seen a hint of the funnel of unburned gas in the middle of the flame. There is a darker area in the middle of the flame. The flame propagates from right to left. Time of picture is 0.114 sec.

Figure 4.19: The flame front has a wavy front. Time was $t = 0.115$.

wave passed the flame front and halted it once more. This time it was unclear from the film if the flame inverted, but the flame front was almost sinusoidal, see figure 4.19. This could be interpreted as two small funnels at approximately half the pipe radius, or a collapse of the earlier funnel. This phenomena appears at time 0.115 sec., 5 ms after the first stop and 1 ms after figure 4.18. Inside the funnel the gas flows from left to right, i.e. into the flame and the funnel. It was expected to see instabilities of the flame inside the funnel due to Kelvin-Helmholzt instabilities, but it was not visible on the film. There was also no sign of Rayleigh-Taylor instabilities when the pressure waves propagated through the flame from behind. While the Landau-Darrieus instability could likely cause the growth of funnel instabilities, even though the properties inside the pipe doesn't satisfy the semi incompressible assumption.

The flame propagated further with hints of two funnels and halted again at $t = 0.117$ sec. The flame halted again at $t = 0.119$ sec. and at $t = 122$ sec. At this point the flame was right in front of the obstacle. The expansion behind the flame forced the unburned gas in front of the flame to form a jet through the 30 mm opening in the obstacle. When the flame passed through the obstacle the jet of reactants burned and due to the high turbulent intensity a large energy release caused a local explosion in the jet sending pressure wave back into the transparent pipe, this explosion was not filmed (it was in the steel tail pipe), but it was likely to assume that it in fact happened. This assumed local explosion might be caused by induction time gradients and may be a failed DDT. The pressure waves were clearly visible an the film. Assumptions was based upon pressure and time recordings, which showed that the highest pressure peak was first recorded on sensor 3 in the tail pipe before in was recorded on sensor 2 and 1 inside the transparent pipe. These pressure waves might even be shock waves, but due to assumed slow rise time of the Kistler 7001 pressure transducer, it was not explicitly concluded that the waves in fact was shock waves. The rest of the unburned gas burned in the steel pipe and on the outside of it. This experiment followed the most logic history of event, where the highest release of energy was in the jet behind the obstacle. Later experiments revealed that a local explosion likely happened before the obstacle.

4.4.2 Event history of experiment 10 with 35% H_2 concentration

There are several possible explanations to what happened in this experiment. Two different explanations will be given in this section. The different explanations explains the last part of the flame propagation just before the flame passed through the obstacle, and governs the sequence of the pressure peaks.

The first part of this experiment was the same as the 30% H_2 experiment. The flame propagated a little bit further before it halted, but there was only vague hints of inversion formation. There was some slightly darker areas which can be interpret as inversion, but it was not as clear as experiment 9. When the flame continued to propagate it continued until it halted again and the front of the flame got a bubble shape in front. This bubble could be caused by Rayleigh-Taylor instabilities where the light products accelerate into the denser reactants, but it was assumed to be three dimensional effects of the flame or effect of inversion collapse. One difference between this and the earlier experiment was that the flame only stopped twice before the obstacle. The flame propagated faster and had higher pressure build up. This was likely caused by the higher laminar burning velocity of rich hydrogen mixtures than stoichiometric mixtures [9].

The most interesting difference between the earlier experiment and this experiment was the order of the pressure peak. In this experiment the first high pressure peak was recorded on sensor 2 inside the pipe, contradicting the first recorded peak behind the obstacle in experiment 9. The next peak was recorded on sensor 1 in the closed ignition end before it was recorded a pressure peak behind the obstacle. The time from the peak on sensor 2 until the peak on sensor 1 was 0.9 ms., this corresponds to wave speed of 1052 m/s. This implies that a local explosion happened before the obstacle. It was not visible from the film where the explosion happened because it was behind the 70 mm long flange attached to the Lexan pipe. The local explosion could be caused by pressure build up in the corner between the pipe wall and the steel flange and induction time gradients. Detonations are often recognized by sudden pressure increase, but again the assumed slow rise time of the Kistler 7001 pressure transducer might not record a detonation. The pressure build up could have caused a hot spot, and induction time gradient in the corner. Increased turbulence generation due to circulating flow in the corner could be an other explanation to the increased burning rate and energy release. After the pressure peak was recorded on sensor 2 and sensor 1, it was recorded a pressure peak on sensor 3 in the tail pipe. This pressure peak might origin from the same explosion as the peaks recorded on sensor 2 and 1, but it might also be caused by an other explosion in the highly turbulent jet through the obstacle.

An other possible explanation to the phenomena was the propagation of an assumed shock waves passing the flame from behind and reflecting. Before the top pressure peaks, the travelling waves in the pipe sharpened and could have become a shock wave, see figure 4.14 (sensor 1). When this shock reflected at the ignition end, it passed through the flame some where between sensor 2 and the obstacle. When the shock hit the flame from behind it reflected but also passed through it. This can explain the two step pressure increase in figure 4.15 as well as the pressure oscillations after the peak before it reduces again. The first pressure increase was the shock moving from right to left. The second

increase was the shock reflected at the flame and the oscillations after that was the that passed the flame and was reflected at the obstacle and moved through the highly wrinkled flame. After this the shock reflected once again at sensor 1 before the flame ignited the jet through the obstacle and exploded behind the obstacle.

4.4.3 Event history of experiment 12 with 40% H_2 concentration

This experiment also follows the same initial steps as experiment 9 and 10. Experiment 12 does however have a different sequence of pressure peaks than both experiment 9 and experiment 10. Higher pressure was likely due to higher laminar burning velocity at 40% H_2. The different order of pressure peak indicates that, no matter which of the earlier explanations, the phenomenon moved to the right. The high speed film of this experiment was of poor quality. In this experiment there was several phenomena happening at the same time.

First the shock waves hit sensor 2 and reflected but soon after the flame produced a new strong pressure wave, possibly due to collapse of an inversion. This new pressure wave was recorded on sensor 2 0.3 ms after the earlier one. At his point there was likely two waves moving towards sensor 1. When the first reflected at the closed end it hit the second one and a new wave propagated towards sensor 2 and passing the flame somewhere between sensor 2 and the obstacle. After this the jet started burning and an explosion in the jet or possibly in the obstacle sent a wave passing sensor 2 and then it hit sensor 1. It was indications that there could have been several explosions in the jet.

There was also a possibility of local explosion in the pipe before the obstacle, referring to the first proposed event history of experiment 10. The gas could have exploded sending pressure waves towards sensor 2 and 1. A reflected wave hit sensor 2 again before the jet caught fire and sent pressure waves into the pipe, at this point it could have been two waves propagating inside the pipe.

In both the 35% and the 40% experiment there is a need to further investigate if there are only one, or more flame fronts due to local explosions ahead of the main flame.

Chapter 5

CFD simulations

The experiments clearly showed a linkage between pressure peaks reflected at the obstacle and halted propagation of the flame. The was also quite evident that the flame inverted when the pressure wave hit the flame. But the flame did not invert every time the pressure wave hit the flame. The process of flame inversion is still quite unclear and needs a further investigation. The following chapter has focus on just flame inversion since simulation of the whole pipe is done by Vågsæther and Bjerketvedt earlier [1]. The simulations is done with shock waves for simplicity. One very useful tool for investigating this effect is CFD methods. When simulating a flow phenomena using CFD methods, it is easy to eliminate unwanted effects and mechanisms. The basics of CFD methods is to solve discretized transport equations in a distributed mesh.

The CFD method used for the thesis is the FLIC (Flux Limiter Centred Scheme) which combines the *FORCE* scheme and the Richtmyer scheme. The details of the FLIC method will not be discussed in this thesis. For further details about the FLIC code see [22].

This chapter is organized with a section with a proposed mechanism for flame inversion, later a section with selected equations used in the simulations. Further are the simulations and a discussion linking the simulations and experiments.

5.1 Inversion due to pressure wave and non planar flame interaction

Since there was several incidents of flame inversion during the flame propagation in the experiments, there is a need to further investigate the phenomenon. It's assumed that shock waves passing through a planar flame causes earlier mentioned Richtmyer-Meshkov instabilities. Inversion of the flame is assumed to be caused by acoustic and/or shock waves passing through a non planar flame and generating radial pressure gradients.

When a pressure wave passes through the front of the flame, see figure 5.1 the center of the shock or acoustic wave will propagate faster in the products than in the surrounding reactants. This difference in wave speed will in turn propagate as a semi hemisphere, but at the same time there will be negative pressure gradients along the radius. This is very evident when there is shock waves propagating through the non planar flame front. The generated pressure

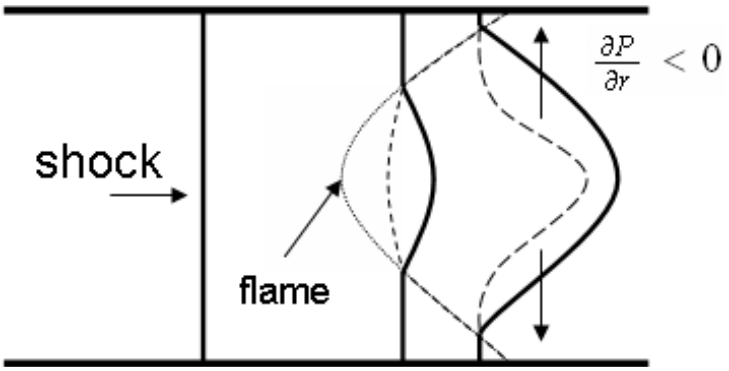

Figure 5.1: Sequenced illustration of how non planar flame front interact with pressure waves. The figure shows three different time instances. The pressure wave creates pressure gradients in the radial direction. These gradients generates flow in the radial direction as well.

gradients will cause the products to flow radially from the center of the pipe. It will flow towards the wall but also stagnate after a while. The flame is still burning, but in the funnel caused by the inversion the flame burns towards the center of the pipe. The flow in front of the flame will also stagnate in the funnel, and it is expected that the flame will propagate in the order of the laminar burning velocity when burning in the funnel towards the center of the pipe. The mechanism of Landau-Darrieus will influence the growth of the funnel when the flame front has changed from convex to concave shape. Both acoustic waves and shock waves are assumed to cause this phenomena of inversion initiation, but there have to be a certain strength of the waves. It is possible that there are certain critical wave strengths that causes inversion.

There is also a possibility that pressure waves passes through inverted flames, and a possible outcome of that scenario will be presented. The principle behind pressure wave interaction with inverted flames are much the same as with non planar finger shaped flames as presented earlier. The waves propagate faster in the products than in the reactants. These differences causes radial pressure gradients and flow from high pressure towards low pressure region. The assumed outcome from pressure or shock wave interaction with inverted flames is presented in figure 5.2.

As shown there is a possibility that pressure waves causes the inversion of the flame but at the same time it is also possible that the collapse of the inversion funnel also is caused by propagating pressure waves. Further investigation of these phenomena is required to fully understand the mechanics of flame inversion due to wave interaction. CFD methods are a good way to investigate such effects, since it is possible to eliminate other influencing factors.

5.2 Mathematical model

These equations are often called the conservation equations and are based upon elemental laws of physics. These laws are the conservation of mass, Newtons

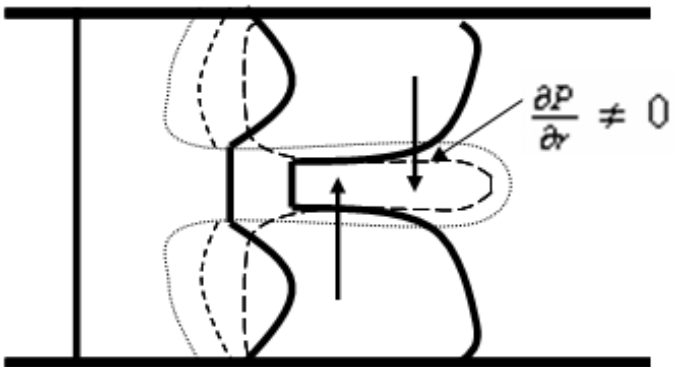

Figure 5.2: Illustration on how wave interacting with inverted flame could evolve. The illustration is given for three different time instaces.

second law as conservation of momentum, and the first law of thermodynamics governing the change of energy is the sum of heat added and work done. The equations are used to model combustion and flow phenomena. In contrast to the Navier-Stokes equations the Euler equations does not govern any diffusion processes.

$$\frac{\partial \rho}{\partial t} + \nabla \cdot (\rho U) = 0 \tag{5.1}$$

$$\frac{\partial \rho U}{\partial t} + \nabla \cdot (\rho U U^T) + \nabla P + \nabla \cdot \widehat{\boldsymbol{\tau}} = 0$$

$$\frac{\partial \rho E}{\partial t} + \nabla \cdot (U(\rho E + P)) + \nabla \cdot (U \cdot \widehat{\boldsymbol{\tau}}) = 0 \tag{5.2}$$

Where U is the velocity vector, ρ is mass density, P is pressure, $\widehat{\boldsymbol{\tau}}$ is the stress tensor. The energy E is the sum of internal, kinetic and chemical energy.

$$E = \frac{P}{(\gamma - 1)\rho} + \frac{1}{2} U \cdot U + q\beta \tag{5.3}$$

Where γ is the ratio of specific heats, q is heat release per unit mass and β is a reaction progress variable and can be expressed as a dimensional less conservation of a specie. For hydrogen it can be.

$$\beta = \frac{[H_2] - [H_2]_{burned}}{[H_2]_{unburned} - [H_2]_{burned}} \tag{5.4}$$

The reaction progress variable β is transported just like other variables in the system and therefore. And the rate of change of β is equal to the rate of reaction.

$$\frac{\partial \rho \beta}{\partial t} + \nabla \cdot (\rho \beta U) = \dot{r}_x \tag{5.5}$$

The rate of reaction is given as:

Property	unit	Value
δx and δr	mm	0.5
Length	mm	350
Radius	mm	48.5
Number of cells	-	97000
M_w reactants	kg/mol	$20.9114e-3$
M_w prod.	kg/mol	$24.0832e-3$
P_0 (initial pres)	Pa	$1e5$
$\gamma_{unburned}$	-	1.401
γ_{burned}	-	1.244
ϕ equivalence ratio	-	1
q energy release	J/kg	$3.2e6$
cfl	-	0.9

Table 5.1: The simulation settings

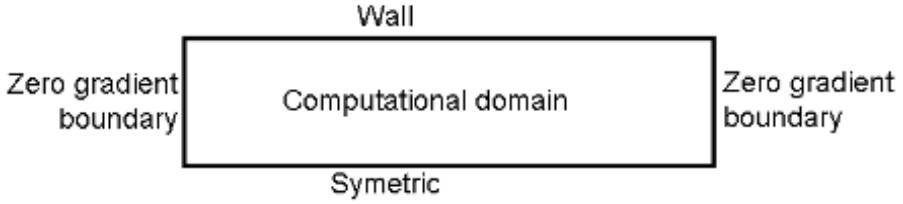

Figure 5.3: A stetch of the computational domain and the boundary conditions.

$$\dot{r}_x = \max\left[\rho_u S_T \left|\nabla\beta\right| \ , \ r_k\right]$$

Where ρ_u is mass density of reactants, S_T is the turbulent burning velocity. The first argument of $\dot{r}_k$ is reaction progress variable rate of reaction and r_k is an Arrhenius type rate of reaction.

5.3 Initial simulation

The general setting for the simulations is shown in table 5.1.

Besides these settings the general mesh is 2D cylindrical with lower boundary as center of the pipe. A sketch of the computational domain is given in figure 5.3.

Detailed investigation of flame inversion due to pressure wave interaction is hard to investigate in experiments since it is very hard to isolate effects. CFD methods are good methods which gives detailed information with regards to several parameters otherwise impossible to record from experiments. The goal of these simulations is to investigate how shock waves interact with flames and if they causes inversion, but also if shock waves collapses already established funnels.

A convex flame was established as initial condition for the simulation. Convex flames are convex towards the reactants. The convex flame was created by

initially having a inclined flame and simulating until it got the right shape with an established flow field behind it. Initially the flame propagated from right to left with a closed boundary on the right hand side. The left boundary was open with zero gradient pressure. No obstacle was present in the simulation. Details governing the simulation parameters are given in the table above.

Shock wave interaction with flame fronts was initially simulated using a closed right boundary, but reflections of the shock wave at the closed end caused complex flow and it was hard to isolate the effects of shock waves moving from left to right, since the reflecting waves interfered. The system was transposed to have both ends open, and a constant velocity was added to the whole system so the flame did not move outside the computational domain. A moving reference system was also used to avoid the flame moving out side the domain.

5.4 Results

The results from CFD simulations are often highly detailed regarding many properties. In this chapter only the properties regarded as highly interesting will be presented.

This simulation started initially with a convex flame with a developed flow field in front and behind it. Just in front of the flame, the properties where changed to simulate a shock of strength Mach 1.2. Figure 5.4 clearly shows how the shock wave interact with the flame. The contour plot of the pressure shows how the shock propagates faster in the products than in the reactants, and that it reflects of the top wall. The figure also shows how it generates a radial flow of gas. It is also shown that the radial velocity is high in some areas behind the shock wave.

Further simulation shows that the flame front inverts further after the shock wave has passed through the flame.

Figure 5.5 shows the process of flame inversion from the simulations. The funnel is created long after the shock wave passed through the flame. To investigate how the funnel is created, the flow field ahead of the flame must be investigated.

When the shock waves passes through the flame it generates a radial flow, and there is an expansion behind the flame. The expansion will drag the center of the flame backwards, thus creating the funnel.

Figure 5.6 shows how the shock wave generates a radial flow behind the flame, and the diverging flow line indicates an expansion behind the center of the flame. It's also visible that the flow in from of the center of the flame converges and thus the flame is unstable according to the same mechanisms as the Landau-Darrieus mechanism. The flame cannot be considered laminar and the assumption of semi incompressible (only density change across the flame) does not hold due to high velocities. The funnel increases in length with further simulation and does not change back to the convex shape as the initial flame.

5.4.1 Collapse of the funnel

The experiments indicates that the funnel collapses and the flame change back to a convex shape. It's proposed that a new pressure wave could lead to the collapse and change of curvature. This phenomena has been studied by simulation. The

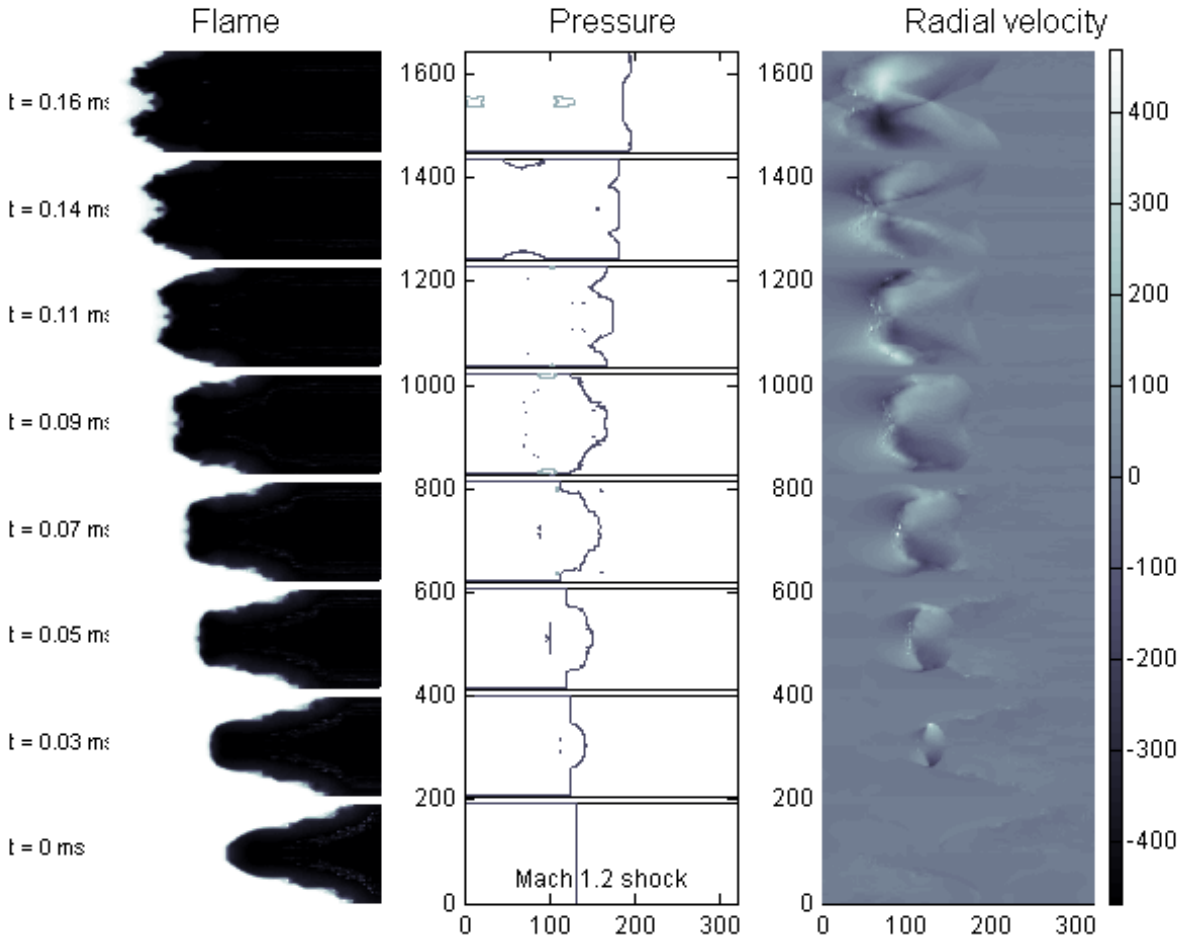

Figure 5.4: Shock wave (Mach 1.2) interaction with a convex flame front. Illustration of the flame front and a contour plot of the pressure to illustrate how the shock propagates with different velocity in the products and reactants. The radial velocity is also shown to illustrate the local spots of high radial flow velocity. The velocity displays the radial direction both positive and negative, so it could be interpred as a 2D cartesian figure.

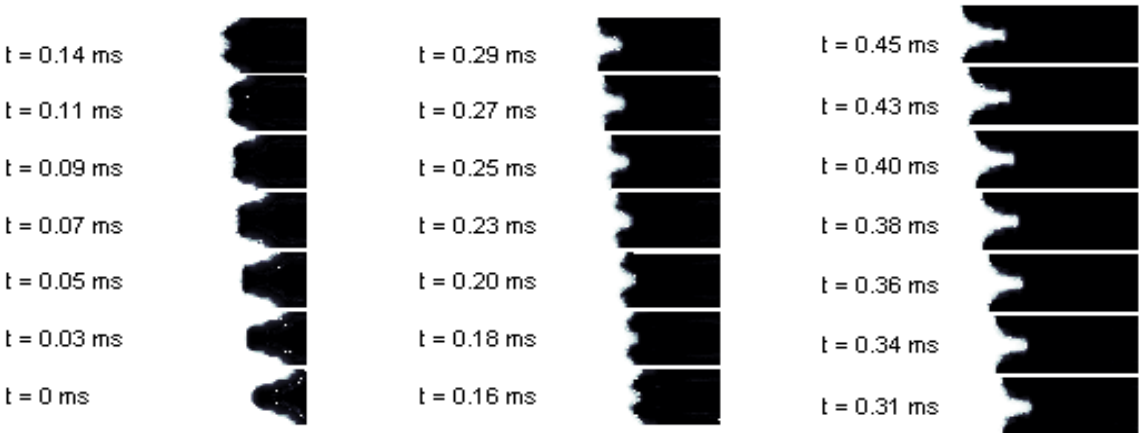

Figure 5.5: Shock wave (Mack 1.2) interaction with a convex flame front. Here the flame front is shown for every 40th timestep of the simulation. The whole flame is shown and it's clear to see how the flame inverts and a funnel of reactants is formed inside the flame front.

Case	Shock direction	Shock strength	Changes curvature back to convex
1	react. to prod.	Mach 1.2	No
2	react. to prod.	Mach 1.4	Yes
3	prod. to react.	Mach 1.2	No
4	prod. to react.	Mach 1.4	No
5	prod. to react.	Mach 2.2	No

Table 5.2: Case matrix of the simulations with shock waves propagating through an inverted flame

proposed collapse mechanism is a pressure wave passing through an inverted flame front from the reactants. Five different cases has been studied and shown in table 5.2.

A second shock passing through the inverted flame generates pressure gradients in the opposite direction than when passing through a convex flame. The flow towards the center of the pipe in not visible in all pictures, there is also large eddies near the walls in the simulated results, see figure 5.7. The flow lines are visualized, even though the flow is compressible. There are also a higher density of flow lines in the center of the visualizations, this is done to give more detail description of the flow in and behind the funnel.

The time steps for case 1 is shown in table 5.3.

The Mach 1.2 shock (case 1) shown in figure 5.7 does not cause the flame to change curvature back to convex shape. There are oscillating pressures in front and behind the funnel.

Figure 5.8 shows the further flame development of case 1. The shock is not strong enough to change the curvature of the flame back to convex shape, and a Landau-Darrieus like mechanism is believed to invert the flame from frame 60 to frame 80. The flow velocity in front of the funnel is lower than the velocity in front of the flame closer to the wall, hence the flame will burn relatively to

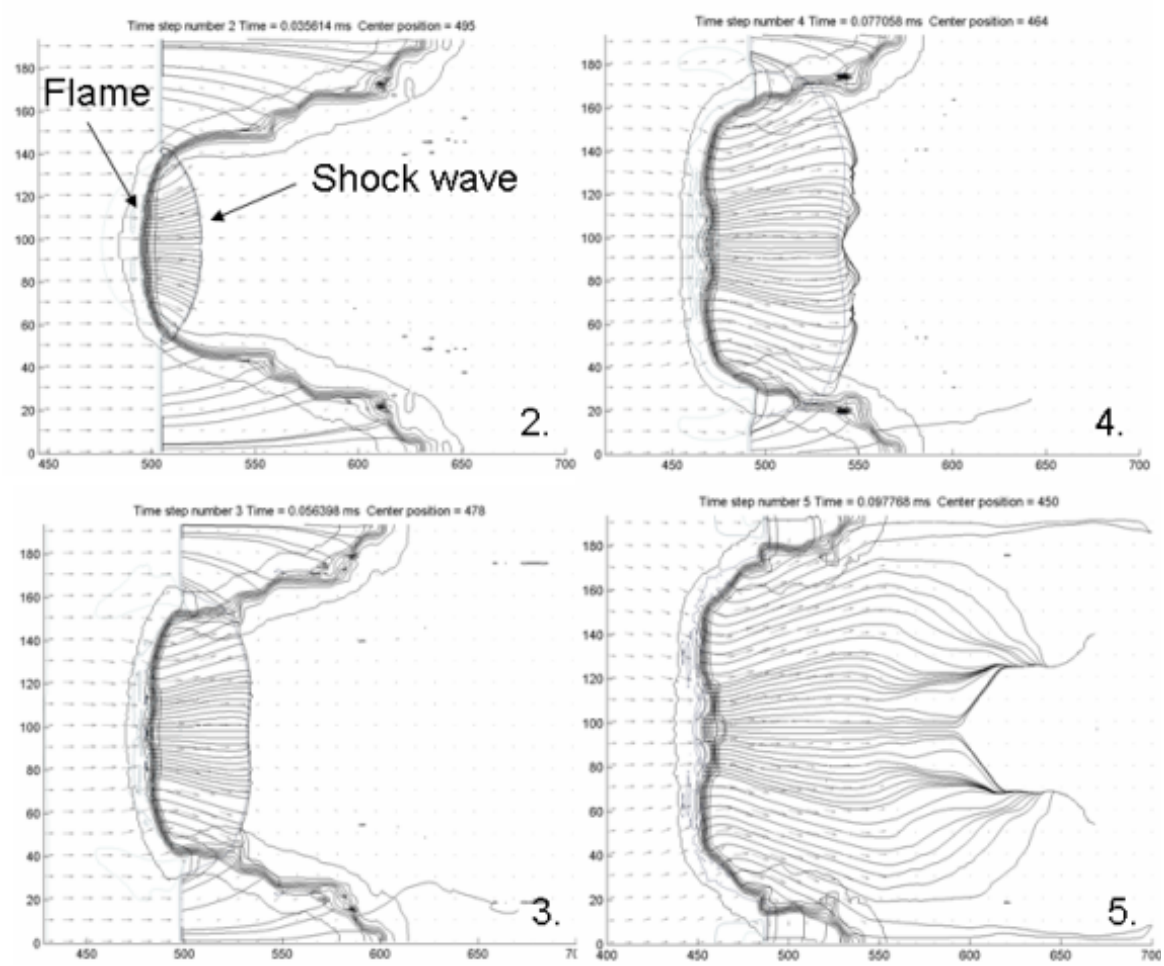

Figure 5.6: Shock wave (Mack 1.2) interaction with a convex flame front. Visualizing the velocity vector and stream lines together with contours of the flame and the pressure. This is the first shock of Mach 1.2 passing through a convex flame. Frame 2 = 0.036 ms, Frame 3 = 0.056 ms, Frame 4 = 0.078 ms and Frame 5 = 0.098 ms.

Case 1	Shock strength Mach 1.2
Frame	**Time [ms]**
22	0.478
23	0.502
24	0.525
25	0.547
30	0.652
40	0.862
60	1.413
80	2.024

Table 5.3: The time steps of the figures in case 1

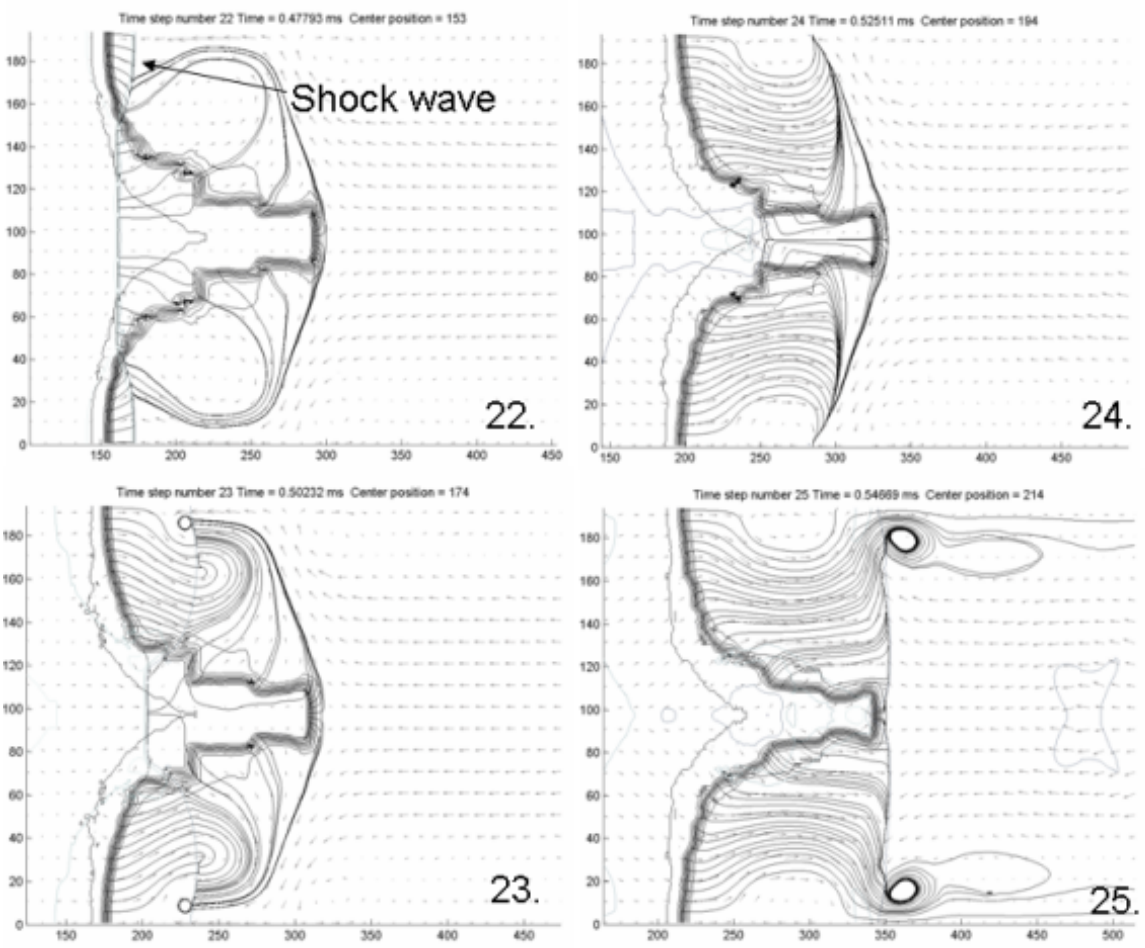

Figure 5.7: Case 1 shock wave (Mach 1.2) interaction with the inverted flame front. A second shock of strength Mach 1.2 passing through an inverted flame-front.

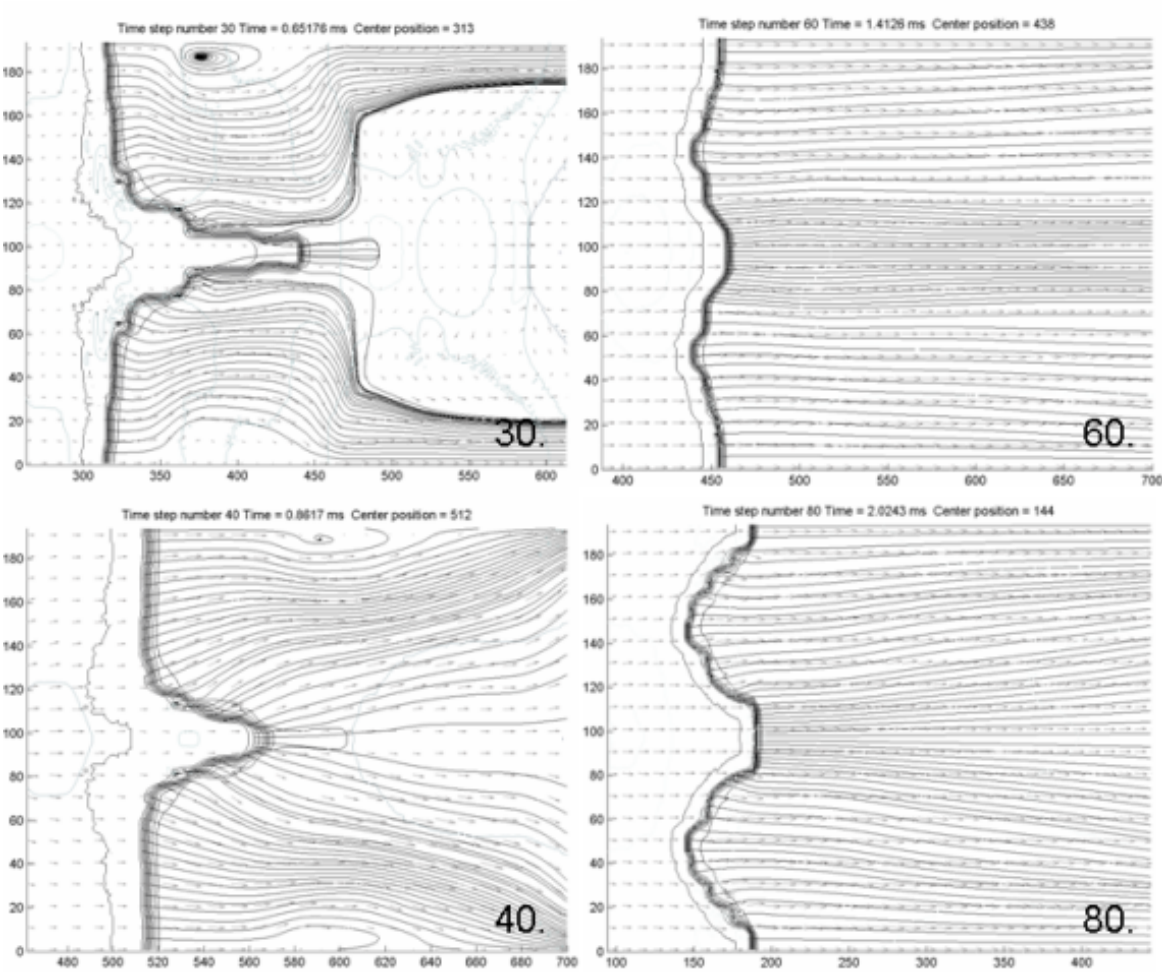

Figure 5.8: Case 1 shock wave (Mach 1.2) interaction with the inverted flame front. This figure shows how the flame almost changes curvature back to convex shape.

Figure 5.9: Case 2 Mach 1.4 shock wave propagating from reactants to products through the inverted flame. Black part is the products. The sequence showes that flame front changes from inverted back to convex shape.

the right in the center.

A shock of strength Mach 1.4 collapsed the funnel and changed the curvature back to convex shape. A sequence of flame fronts of case 2 is showed in figure 5.9. The shape of the flame is changed long after the shock wave has propagated through the flame. This indicates that the shock wave only initiates the changes of curvature.

A figure displaying the details from the simulation is shown in figure 5.10. The shock wave creates the proposed flow, but there is also change of flow ahead of the flame. The flow diverges for some time and the flow velocity is also decreased. This might be caused by a stagnation of products behind the flame. The results are not precise in defining the dominant mechanism of the collapse of the funnel. As the shock wave propagates faster in the products than in the reactants it is possible that a zone of not shocked reactants in the bottom of the funnel is surrounded by shocked gas on all sides. This low pressure zone in the bottom of the funnel is assumed to be a contributing factor of the collapse. Once the flame has a convex curvature, it is stable for a reasonable time. Frame 25 and 28 clearly shows that the flow diverges and slows down in front of the funnel. It is also evident that the shock wave changes the flow towards the center of the pipe. The inwards radial flow stagnates with the products from the flame, see figure 5.10 (frame 28). This stagnation might force the funnel to collapse.

A shock from behind the flame does not cause collapse of the funnel and change of curvature. Three different shock strengths was investigated, Mach 1.2 (case3), 1.4 (case 4) and 2.2 (case 5). One common phenomena of the three simulations is the reflection of the shock in the flame. The shock both propagates through the flame and reflects back. This effect causes flow in both directions. The Mach 1.2 shock (case 3) from behind does not influence the flame very much, the funnel becomes longer, most likely due to Landau-Darrieus like mechanisms of converging and diverging flow in front of the flame.

The Mach 1.4 shock (case 4) influences the flame much more, and changes the shape of the funnel. It does not however change the curvature of the flame back to convex shape. The funnel is shortened when the shock wave passes

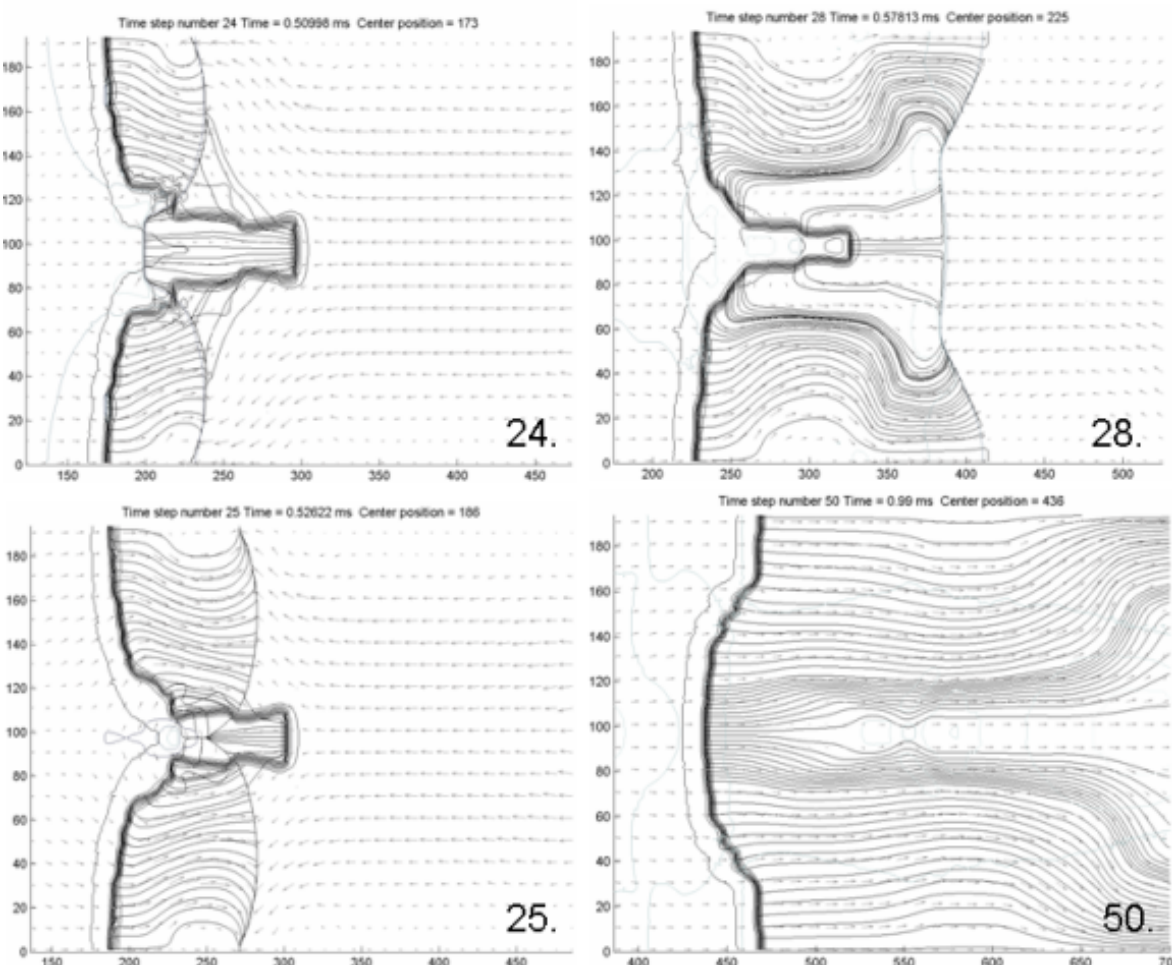

Figure 5.10: Case 2 shock wave (Mach 1.4) interaction with the inverted flame front. This is sufficient to change the curvature back to convex shape. Frame 24 = 0.510 ms, Frame 25 = 0.526 ms, Frame 28 = 0.578 ms and Frame 50 = 0.990 ms.

through from the products and generates a relative flow from products towards the flame. When the shock wave is reflected at the flame it stretches the funnel again. The flow in front of the funnel converges into the funnel and causes higher flow velocities which in turn pushes the funnel into the products. The funnel gets a more triangular shape then earlier. Simulation results are shown in figure 5.11.

A Mach 2.2 shock (case 5) was assumed, before it was simulated, to cause DDT in the funnel due to mechanism of induction time gradients. This was assumed because the temperature inside the funnel was quite high before any shock passed through it. The simulation did not detonate, and it did not change curvature back to convex shape. The funnel almost caught up with the front part of the flame, but the simulation ended with a growth of the funnel.

5.5 Discussion

The simulated phenomena of inversion and the experimental results shows several resemblances which needs discussion. The pressure records shows that the flame countermarches and sometimes inverts when pressure waves passes through the flame. This part will focus on the linkage between experiments, theory and simulations.

Flame inversion was quite evident in the experiments, and figure 4.11 clearly shows a relation between waves reflected at the obstacle and countermarch of the flame. The high speed film also shows that the flame inverts when the first wave hits the flame from the reactant side, see figure 4.6 and 4.7. It is known from the theory of Landau-Darrieus instabilities that a flame with concave parts will be unstable, the assumption of semi incompressibility does however not hold for the experiments, but the phenomena of converging flow in front of concave parts of the flame is observed in simulations.

Experiments show that the flame sometimes inverts when hit by a pressure wave, simulations have described in detail how it's done with waves propagating faster in the products than in the reactants, and how this generates a radial flow on products which initially changes the curvature of the flame tip. A change of curvature caused by pressure waves, initiates the inversion of the flame. The Landau-Darrieus mechanism together with low pressure zones behind the flame, generated by the expansion behind it, fulfills the inversion of the flame. It's fully plausible that a shock wave or maybe also an acoustic wave could cause initiation of flame inversion.

Experiment number 9 with 30% hydrogen showed that the flame inverted after a pressure peak was recorded at the obstacle (approx. 0.111 sec.). The pressure wave was reflected at the obstacle and passed through the flame from the reactant side, and thus inverting the flame. When the next pressure peak was recorded (approx. 0.115 sec.) the inverted flame collapses, see figure 4.6.

Experiment number 10 with 35% hydrogen shows in figure 4.6 that the flame has an bubble shaped front. This shape is also seen in the simulations in figure 5.10 and frame 50. The bubble shape appears after the second pressure peak, which highly underline the collapse of an already established funnel created by the first pressure peak. Experiment number 9 in figure 4.8 in frame 7 shows hints of the same bubble shape. The time at which the hint of the bubble shape appears corresponds to the second pressure peak. The bubble shape appears in

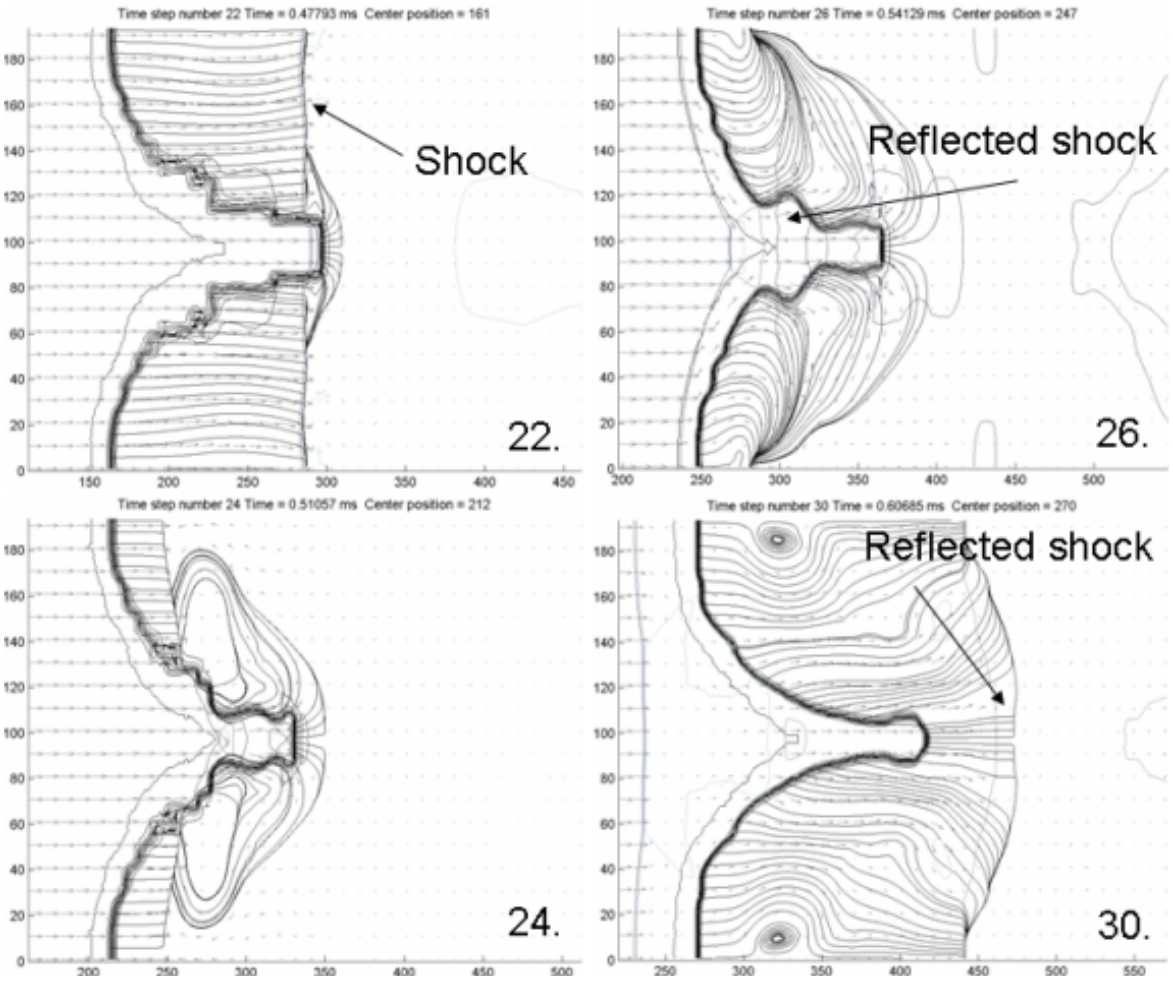

Figure 5.11: Case 4 shock wave (Mach 1.4) interaction with the inverted flame front. Shock wave propagates from products to reactants. The shock reflects at the flame, and does not change the curvature of the flame. Frame 22 = 0.478 ms, Frame 24 = 0.511 ms, Frame 26 = 0.541 ms and Frame 30 = 0.607 ms.

experiment number 11 with 35% as well.

Simulations shows that shock waves propagating from products through the flame, both reflects at the flame and propagates through. Even strong shock waves, Mach 2.2, does not change the curvature of inverted flames back to convex shapes. The experiments also shows the same results.

There are in general good correspondence between the simulations and the experiments. The effects of inversion occur similarly in simulations and experiments. The collapse of the funnel in the simulations are in good accordance with the experiments as well. The bubble shape are clearly visible in both simulations and some experiments. There are some effects in the experiments which are removed in the simulations. Heat loss through the pipe wall is not present in the simulations, but not thought to influence very much since the time scale of one shot is very short. It's however suggestive to investigate this effect further.

As a general discussion issue, the experiments should have been conducted with more patient. The filling time of 2 min, corresponding to filling the pipe twice could very well be too short. For further experiments the filling time should be investigated.

Chapter 6

Conclusion

The tasks of this report was to do litterateur research, experiments and simulations of hydrogen explosion in a pipe with a single obstruction. The background and motivation for the work was based on earlier experiments and simulations done by Vågsæther, Bjerketvedt and Knudsen [1, 2]. There was a need to verify flame inversion not observed earlier in experiments. There was done several experiments in the laboratory at Telemark University College. Simulations where calculated using a FLIC code written by Vågsæther.

The work of this main thesis has raised many questions. The main conclusion could very well be to further investigate the phenomena of flame propagation in pipes, both in experiments and simulations.

Experiments of hydrogen explosions in a transparent pipe with a single obstacle shows that the flame inverts one ore more times before the flame passes through the obstacle. It is rather hard to determine with absolute certainty that the flame inverts, but high speed film of the experiments gives good indications of flame inversion. There is a clear connection between halted propagation (and sometimes inversion) and acoustic waves propagating from reactants through the flame. The flame halts and sometimes inverts when hit by an acoustic wave. There is also proposed an explanation of the phenomena, where the main element initiating inversion is pressure gradients caused by different speeds of sound in reactants and products.

CFD simulations of flame inversion supports the proposed theory, but the simulations has been simplified to govern shock waves rather than acoustic waves. The simulations also show good resemblance between simulations and experiments, even though they differ in type of propagating waves.

The theory of flame propagation starting with ignition, instabilities, turbulent flames and the possibility of DDT is presented in the report. The instability mechanism presented by Landau and Darreius has be given emphasis in this report since it's believed to be of great importance in the case of flame inversion due to propagating pressure waves in a pipe with a single obstruction. The theory of DDT is briefly described and it can be concluded that the mechanisms of DDT is still an unsolved problem of great importance.

Further work in the topic presented in this report should be:

- Experiments investigating the last centimeter of the pipe before the obstruction to reveal what happens there. The use of a square pipe and

schlieren phothage could give more detailed information than a circular pipe without schlieren method. This method should also include phothage of the flow behind the obstacle to reveal the nature of different order of pressure peaks, recorded at the pressure sensors, varying with H_2 concentration. Filling time is also an issue to further investigate

- Further CDF simulations with smaller grid size could reveal other instabilities regarding the flame inversion. It is of great interest to investigate the collapse of the funnel in greater detail. This might unravel more phenomena caused by shock waves propagating with different velocities in reactants and products.

- CFD simulations with a distributed range of shock strength could possibly reveal critical conditions regarding flame inversion.

- Flame inversion caused by acoustic waves should be investigated with CFD methods, to further verifying the CFD code used in this report.

- The possibility of DDT in inverted flames should be investigated further both in experiments and simulations.

A scientific paper draft is given in the appendix. The paper governs the inversion of a convex flame due to shock waves.

Chapter 7

References

1. Vaagsaether K. and Bjerketvedt D. (2007), Simulation of flame acceleration in an obstructed tube with LES, *ICDERS 2007*, Poitiers France
2. Knudsen V., (2006). Hydrogen gas explosions in piplines-modeling and experimental investigations. NTNU Trondheim
3. Mushrooms+Snakes a visualization of Richtmyer-Meshkov instabilities, http://cnls.lanl.gov/~azathoth/cover.html, accessed 2. April 2008
4. Zender C., *Planetary Boundary Layer: Turbulence,* Department of Earth System Science University of California, [online]. Available from http://dust.ess.uci.edu/ess bnd/smn trb.pdf
5. Landau L., (1944), on the theory of slow combustion, *Acta physicochimica URSS 19*, pp 77-85
6. Chomiak J., (1990), Combustion, A study in theory, fact and application, Energy & engineering science series, Abacus Press, ISBN 0 85626 453 9
7. Peters N., (2000). Turbulent combustion. Cambridge university press, ISBN 0 521 66082 3
8. Turns S. R. (2000), An indtroduction to combustion, concepts and applications, second edition, McGraw-Hill International editions, ISBN 0 07 235044 X
9. Liñán A. and Williams F. A., (1993), Fundamental aspects of combustion, The oxford engineering science series, Oxfor university press, ISBN 0 19 507626 5
10. Bjerketvedt D., Bakke J. R., and van Wingerden K., (1997), Gas explosion handbook, Journal of Hazardous MAterials, volume 52, pp 1-150
11. Oran E. S. and Gamezo V. N., (2007), Origins of the deflagration-to-detonation transition in gas-phase combustion, Combustion and flame 148 , Elsevier
12. Urtiew P. A. and Oppenheim A. K., (1966),Experimental observations of the transition to detonation in an explosive gas, Proceedings of the Royal Society of London, Series A, Vol 295, pp 13-28*

13. Breitung W., et. al. (2000), Flame acceleration and deflagration to detonation in nuclear safety, State-of-the-art report by a group of experts, OECD Nuclear Energy Agency NEA/CSNI/R7*

14. Lee J. H., Knystautas R. and N. Yoshikawa,(1978), Photochemical initiation of gaseous detonations, Astronautica Acta, 5, pp 971-982*

15. Teodorczyk A., (2006) Fast deflagrations, deflagration to detonation transition (DDT) and direct detonation initiation in hydrogen-air mixtures, Proceedings of the first European Summer School on Hydrogen Safety, Belfast Ulster

16. Steen H. and Schampel K. (1983), Experimental investigation on the run-up distance of gaseous detonations in large pipes, 4th. International Symposium on Loss Prevention and Safety Promotion in Process Industries, 82 pp E23-E33*

17. He L., (2000), A scaling analysis of the critical conditions for a deflagration-to-detonation transition, Combustion Theory and Modeling, 4, pp 107-122*

18. Lee J. H., Knystautas R. and Chan C. K. (1984), Turbulent flame propagation in obstacle-filled tubes, Proceedings of the combustion institute 20th. pp 1663-1672*

19. Moen I. O., (1993), Transition to detonation in fuel-air explosive clouds, Journal of Hazardous Materials, 33, 159-192, Elsevier Science Publishers B. V., Amsterdam

20. Peraldi O., Knystautas R and Lee J. H., (1986), Proceedings of the combustion institute 21th. pp 1629-1637*

21. Lee J. H., Moen I. (1980) mechanism of transition from deflagration to detonation in vapour cloud explosion. Combust. Sci. 6, pp 359-389

22. Toro E. F., (1999), Riemann solvers and numerical methods for fluid dynamics, Springer-verlag, Berlin

23. Kaneshige M. and Shepherd J. E., (1997), Detonation database. Technical Report FM97-8, GALCIT, July 1997. See also the electronic hypertext version at http://www.galcit.caltech.edu/detn_db/html/.

24. Marble F. E., (1994), Gasdynamic enhancement of nonpremixed combustion, 25th symposium on combustion, The combustion institute.

25. Shengtai L. and Li H,. Parallel AMR Code for Compressible MHD or HD Equations. Los Alamos National Laboratory. [online], Retrieved on 27 may 2008.

26. Maldonado J.D. and Timmes F.X., ZND detonations, [online] available from Cococubed.com, Retrieved on 27 may 2008.

27. Kuo K. K, (1986), Principles of combustion, John Wiley & sons, New York

28. Brown C. J. and Thomas G. O. (1999), Experimental Studies of Shock-Induced Ignition and Transition to Detonation in Ethylene and Propane Mixtures, The Combustion Institute

29. Teerling O. J., McIntosh A. C., Brindley J. and Tam V. H. Y.,(2005), Premixed flame response to oscillatory pressure waves, Proceedings of the Combustion Institute 30, pp 1733-1740, Elsevier Science Publishers

30. Markstein G. H., (1957), A shock-tube study of flame front-pressure wave interaction. Proceedings of the Combustion Institute 6, pp 387-398, Elsevier Science Publishers

References marked with * are referred to as they are discussed in [2]

Appendix A

Draft Report for Shock Waves, Springer Verlag

Remark 1 *This is a draft paper and must be corrected and improved befor publishing. The figures are not of satisfactory quality and format. The introduction and background needs more work espesially referring to other experiments and other simulations. The paper also fucuses on the influence of just shock waves. There are just two cases presented in the paper. One case with shock wave propagating through a convex flame and initiating the inversion. And one case of collapse of the inversion.*